
NEARLY MINIMAX OPTIMAL ADVERSARIAL IMITATION LEARNING WITH KNOWN AND UNKNOWN TRANSITIONS*

A PREPRINT

Tian Xu^{†1}, Ziniu Li^{†2}, and Yang Yu^{1,3,4}

¹National Key Laboratory for Novel Software Technology, Nanjing University, Nanjing 210023, China

²Shenzhen Research Institute of Big Data, The Chinese University of Hong Kong, Shenzhen, Shenzhen 518172, China

³Pazhou Lab, Guangzhou, 510330, China

⁴Polixir.ai

xut@lamda.nju.edu.cn, ziniuli@link.cuhk.edu.cn, yuy@nju.edu.cn

June 22, 2021

ABSTRACT

This paper is dedicated to designing provably efficient adversarial imitation learning (AIL) algorithms that directly optimize policies from expert demonstrations. Firstly, we develop a transition-aware AIL algorithm named *TAIL* with an expert sample complexity of $\tilde{\mathcal{O}}(H^{3/2}|\mathcal{S}|/\varepsilon)$ under the known transition setting, where H is the planning horizon, $|\mathcal{S}|$ is the state space size and ε is desired policy value gap. This improves upon the previous best bound of $\tilde{\mathcal{O}}(H^2|\mathcal{S}|/\varepsilon^2)$ for AIL methods and matches the lower bound of $\tilde{\Omega}(H^{3/2}|\mathcal{S}|/\varepsilon)$ in [Rajaraman et al., 2021] up to a logarithmic factor. The key ingredient of TAIL is a fine-grained estimator for expert state-action distribution, which explicitly utilizes the transition function information. Secondly, considering practical settings where the transition functions are usually unknown but environment interaction is allowed, we accordingly develop a model-based transition-aware AIL algorithm named *MB-TAIL*. In particular, MB-TAIL builds an empirical transition model by interacting with the environment and performs imitation under the recovered empirical model. The interaction complexity of MB-TAIL is $\tilde{\mathcal{O}}(H^3|\mathcal{S}|^2|\mathcal{A}|/\varepsilon^2)$, which improves the best known result of $\tilde{\mathcal{O}}(H^4|\mathcal{S}|^2|\mathcal{A}|/\varepsilon^2)$ in [Shani et al., 2021]. Finally, our theoretical results are supported by numerical evaluation and detailed analysis on two challenging MDPs.

1 Introduction

Reinforcement learning (RL) [Sutton and Barto, 2018] learns the optimal policy from trial and error in unknown environments and suffers from the sample efficiency issue in practice [Mnih et al., 2015, Lillicrap et al., 2016]. On the other hand, imitation learning (IL) [Pomerleau, 1991, Abbeel and Ng, 2004, Ross and Bagnell, 2010, Ho and Ermon, 2016] directly optimizes policies from expert demonstrations, which is more sample-efficient and has been successfully demonstrated in game playing [Ross et al., 2011, Silver et al., 2016], natural language processing [Daumé et al., 2009, Chang et al., 2015], recommendation system [Shi et al., 2019, Chen et al., 2019], and robotics control [Levine et al., 2016, Finn et al., 2016], etc.

The target of IL is to minimize the policy value gap between the expert policy and the imitated policy [Ross and Bagnell, 2010, Xu et al., 2020, Rajaraman et al., 2020]. Representative IL methods include behavioral cloning (BC) [Pomerleau, 1991, Ross et al., 2011] and adversarial imitation learning (AIL) [Abbeel and Ng, 2004, Syed and Schapire, 2007].

[†]: equal contribution.

*: This work is supported by National Key R&D Program of China (2020AAA0107200), NSFC (61876077), and Collaborative Innovation Center of Novel Software Technology and Industrialization. Correspondence to: Yang Yu.

Behavioral cloning aims to imitate the expert policy distribution. Concretely, BC utilizes supervised learning to minimize the action probability discrepancy over states observed in expert demonstrations. Adversarial imitation learning follows the principle of state-action distribution matching [Abbeel and Ng, 2004, Syed and Schapire, 2007, Ho and Ermon, 2016]. It solves a minimax problem: the learner infers an adversarial reward function to maximize the policy value gap and subsequently learns a policy to minimize the policy value gap with the recovered reward function. Based on the above two principles, many practical algorithms [Torabi et al., 2018, Brantley et al., 2020, Fu et al., 2018, Ho and Ermon, 2016, Ke et al., 2019, Kostrikov et al., 2019, 2020] have been developed, and empirical studies suggest that AIL-based algorithms could be better than BC in practice [Ho and Ermon, 2016, Kostrikov et al., 2019, 2020].

Context. This paper focuses on the *sample complexity* and *interaction complexity* of IL approaches, which refers to the number of expert trajectories and interactions with the environment required to achieve a small policy value gap, respectively.

Firstly, when the transition function is known, previous analysis suggests that the sample complexities of BC [Rajaraman et al., 2020] and existing AIL methods¹ (such as FEM [Abbeel and Ng, 2004] and GTAL [Syed and Schapire, 2007]) are $\tilde{\mathcal{O}}(H^2|\mathcal{S}|/\varepsilon)$ and $\tilde{\mathcal{O}}(H^2|\mathcal{S}|/\varepsilon^2)$, respectively, where H is the planning horizon, $|\mathcal{S}|$ is the state space size and ε is the desired policy value gap. This result indicates that AIL is inferior to BC in the worst-case. Recently, Rajaraman et al. [2021] gave the lower bound of $\tilde{\Omega}(H^{3/2}|\mathcal{S}|/\varepsilon)$ for any IL algorithms under the known transition setting and concluded that the MIMIC-MD algorithm [Rajaraman et al., 2020] with the sample complexity of $\tilde{\mathcal{O}}(H^{3/2}|\mathcal{S}|/\varepsilon)$ is nearly minimax optimal. Importantly, Rajaraman et al. [2020] conjectured that “the conventional minimum distance functional (AIL) approach, · · · , does not achieve the rate”, but we still do not know whether AIL can indeed achieve this rate in principle.

Secondly, consider practical settings where transition functions are usually unknown but the environment interaction is allowed, there is no corresponding extension of MIMIC-MD, but several theoretical guarantees of AIL methods are well-known; see Table 1 for a review of previous results. In particular, seminal works [Abbeel and Ng, 2005, Syed and Schapire, 2007] leveraged expert demonstrations rather than interactions to estimate transition function and their algorithms are therefore impractical due to their high sample complexities. To our best knowledge, only Shani et al. [2021] developed the online apprenticeship learning (OAL) algorithm which updates policies and reward functions with optimism, and hence achieved an interaction complexity² of $\tilde{\mathcal{O}}(H^4|\mathcal{S}|^2|\mathcal{A}|/\varepsilon^2)$, where the dependence on H is inferior.

Our Contribution. We work with the adversarial imitation learning (AIL) framework. Firstly, we propose a fine-grained estimator for the expert state-action distribution, inspired by the coupling analysis from [Rajaraman et al., 2020]. The core idea is to utilize the transition function information to refine the estimation. To be more specific, if the transition function is known, we can exactly compute the expert state-action distribution at the observed state-action pairs, instead of estimating it from expert demonstrations like in FEM [Abbeel and Ng, 2004], GTAL [Syed and Schapire, 2007] and OAL [Shani et al., 2021]. Equipped with the fine-grained estimator, a transition-aware AIL approach named *TAIL* is proposed under the known transition setting, which enjoys an improved sample complexity $\tilde{\mathcal{O}}(H^{3/2}|\mathcal{S}|/\varepsilon)$. This upper bound matches the lower bound in [Rajaraman et al., 2021] and hence we deny the conjecture that AIL methods may not be minimax optimal in [Rajaraman et al., 2020].

Secondly, when the transition function is unknown, a model-based AIL algorithm named *MB-TAIL* is correspondingly developed. MB-TAIL builds an empirical transition model in the first place and subsequently implements imitation under the recovered transition model. Since AIL needs to perform policy optimization with different inferred reward functions, we apply a reward-free exploration method [Ménard et al., 2020] to collect trajectories to build the empirical model. Under the unknown transition setting, MB-TAIL achieves an interaction complexity of $\tilde{\mathcal{O}}(H^3|\mathcal{S}|^2|\mathcal{A}|/\varepsilon^2)$, which improves upon the recent result of $\tilde{\mathcal{O}}(H^4|\mathcal{S}|^2|\mathcal{A}|/\varepsilon^2)$ in [Shani et al., 2021].

Finally, we conduct experiments on two challenging MDPs: *Standard Imitation* and *Reset Cliff*, which are adapted from [Rajaraman et al., 2020]. Standard Imitation reveals the statistical estimation difficulty while Reset Cliff highlights the long-horizon challenge. Empirical evaluations demonstrate that the proposed algorithms are efficient compared with existing IL algorithms regarding sample complexity and interaction complexity. We also provide a detailed analysis of the extent of this performance boost. As a byproduct, we empirically verify that the sample complexity bounds of previous AIL methods are tight, which implies that our algorithmic design is indispensable to improve the sample efficiency.

¹In FEM [Abbeel and Ng, 2004] and GTAL [Syed and Schapire, 2007], authors considered the infinite horizon MDP. We translate their results to the episodic setting by replacing the effective planning horizon $1/(1 - \gamma)$ with the finite planning horizon H .

²Shani et al. [2021] proved a regret $\tilde{\mathcal{O}}(\sqrt{H^4|\mathcal{S}|^2|\mathcal{A}|K} + \sqrt{H^3|\mathcal{S}||\mathcal{A}|K^2/m})$, where K is the number of interaction episodes and m is the number of expert trajectories. We convert this regret guarantee into the PAC guarantee considered in this paper by Markov inequality as suggested by [Jin et al., 2018]; see Appendix B for details.

Table 1: Sample complexity and interaction complexity to achieve an ε -optimal policy value gap for different IL algorithms. We use $\tilde{\mathcal{O}}$ and $\tilde{\Omega}$ to hide logarithmic factors.

	Known Transition Setting	Unknown Transition Setting	
	Sample Complexity	Sample Complexity	Interaction Complexity
BC [Rajaraman et al., 2020]	$\tilde{\mathcal{O}}\left(\frac{H^2 \mathcal{S} }{\varepsilon}\right)$	$\tilde{\mathcal{O}}\left(\frac{H^2 \mathcal{S} }{\varepsilon}\right)$	0
FEM [Abbeel and Ng, 2004]	$\tilde{\mathcal{O}}\left(\frac{H^2 \mathcal{S} }{\varepsilon^2}\right)$	$\tilde{\mathcal{O}}\left(\frac{H^2 \mathcal{S} }{\varepsilon^2} + \frac{H^8 \mathcal{S} ^3 \mathcal{A} }{\varepsilon^5}\right)$	0
GTAL [Syed and Schapire, 2007]	$\tilde{\mathcal{O}}\left(\frac{H^2 \mathcal{S} }{\varepsilon^2}\right)$	$\tilde{\mathcal{O}}\left(\frac{H^2 \mathcal{S} }{\varepsilon^2} + \frac{H^6 \mathcal{S} ^3 \mathcal{A} }{\varepsilon^3}\right)$	0
MIMIC-MD [Rajaraman et al., 2020]	$\tilde{\mathcal{O}}\left(\frac{H^{3/2} \mathcal{S} }{\varepsilon}\right)$	-	-
TAIL (Algorithm 1)	$\tilde{\mathcal{O}}\left(\frac{H^{3/2} \mathcal{S} }{\varepsilon}\right)$	-	-
OAL [Shani et al., 2021]	-	$\tilde{\mathcal{O}}\left(\frac{H^2 \mathcal{S} }{\varepsilon^2}\right)$	$\tilde{\mathcal{O}}\left(\frac{H^4 \mathcal{S} ^2 \mathcal{A} }{\varepsilon^2}\right)$
MB-TAIL (Algorithm 2)	-	$\tilde{\mathcal{O}}\left(\frac{H^{3/2} \mathcal{S} }{\varepsilon}\right)$	$\tilde{\mathcal{O}}\left(\frac{H^3 \mathcal{S} ^2 \mathcal{A} }{\varepsilon^2}\right)$
Lower Bound [Rajaraman et al., 2021]	$\tilde{\Omega}\left(\frac{H^{3/2} \mathcal{S} }{\varepsilon}\right)$	$\tilde{\Omega}\left(\frac{H^{3/2} \mathcal{S} }{\varepsilon}\right)$	-

Related Work. Researchers have analyzed IL algorithms based on the *error bound* (i.e., the policy value gap under “infinite” sample setting). Ross and Bagnell [2010] revealed that BC suffers from the compounding error issue, indicating that its error bound is $\mathcal{O}(H^2)$. DAgger [Ross et al., 2011] improves this error bound to $\mathcal{O}(H)$ with active expert queries. By state-action distribution matching, AIL methods also have the error bound of $\mathcal{O}(H)$ [Wang et al., 2020, Xu et al., 2020] without additional expert queries.

Error bound does not fully characterize the sample efficiency of IL methods, which is of interest in practice and theory. Later on, there emerged lots of studies on finite sample complexity analysis to fill this gap [Xu et al., 2020, Rajaraman et al., 2020, 2021]. In addition to results summarized in Table 1, under the unknown transition and no interaction setting, Rajaraman et al. [2020] proved that BC has the sample complexity of $\tilde{\mathcal{O}}(H^2|\mathcal{S}|/\varepsilon)$. This upper bound matches the lower bound of $\tilde{\Omega}(H^2|\mathcal{S}|/\varepsilon)$ under the unknown transition and no interaction setting. Furthermore, under the active setting where the agent can query expert policies when interacting with the environment, Rajaraman et al. [2020] showed that DAgger does not improve the sample complexity compared with BC; see [Rajaraman et al., 2020] for more explanation.

Existing AIL methods (such as FEM [Abbeel and Ng, 2004], GTAL [Syed and Schapire, 2007] and OAL [Shani et al., 2021]) employ a simple maximum likelihood estimator for the state-action distribution of expert policies and do not leverage the transition function information. Hence, their sample complexities do not match the lower bound of $\tilde{\Omega}(H^{3/2}|\mathcal{S}|/\varepsilon)$ in [Rajaraman et al., 2021]. The sample complexity of MIMIC-MD proposed in [Rajaraman et al., 2020] indeed matches this lower bound. However, MIMIC-MD cannot be solved in polynomial time as discussed in [Rajaraman et al., 2020]. Later on, Rajaraman et al. [2021] re-formulated MIMIC-MD as a linear programming problem. Nevertheless, it is still hard to apply MIMIC-MD in IL tasks due to their computation complexity [Lee and Sidford, 2015].

2 Background

Episodic Markov Decision Process. In this paper, we consider episodic Markov decision process (MDP), which can be described by the tuple $\mathcal{M} = (\mathcal{S}, \mathcal{A}, \mathcal{P}, r, H, \rho)$. Here \mathcal{S} and \mathcal{A} are the state and action space, respectively. H is the planning horizon and ρ is the initial state distribution. $\mathcal{P} = \{P_1, \dots, P_H\}$ specifies the non-stationary transition function of this MDP; concretely, $P_h(s_{h+1}|s_h, a_h)$ determines the probability of transitioning to state s_{h+1} conditioned on state s_h and action a_h at time step h , for $h \in [H]^3$. Similarly, $r = \{r_1, \dots, r_H\}$ specifies the reward function of this MDP; without loss of generality, we assume that $r_h : \mathcal{S} \times \mathcal{A} \mapsto [0, 1]$, for $h \in [H]$. A non-stationary policy

³[x] denotes the set of integers from 1 to x .

$\pi = \{\pi_1, \dots, \pi_h\}$, where $\pi_h : \mathcal{S} \mapsto \Delta(\mathcal{A})$ and $\Delta(\mathcal{A})$ is the probability simplex, $\pi_h(a|s)$ gives the probability of selecting action a on state s at time step h , for $h \in [H]$.

The sequential decision process runs as follows: in the beginning of an episode, the environment is reset to an initial state according to ρ ; then the agent observes a state s_h and takes an action a_h based on $\pi_h(a_h|s_h)$; consequently, the environment makes a transition to the next state s_{h+1} according to $P_h(s_{h+1}|s_h, a_h)$ and sends a reward $r_h(s_h, a_h)$ to the agent. This episode ends after H repeats.

The quality of a policy is measured by its *policy value*: $V^\pi := \mathbb{E}[\sum_{h=1}^H r_h(s_h, a_h)|s_1 \sim \rho; a_h \sim \pi_h(\cdot|s_h), s_{h+1} \sim P_h(\cdot|s_h, a_h), \forall h \in [H]]$. To facilitate later analysis, we introduce the state-action distribution induced by a policy π : $P_h^\pi(s, a) := \mathbb{P}(s_h = s, a_h = a|s_1 \sim \rho; a_\ell \sim \pi_\ell(\cdot|s_\ell), \forall \ell \in [h])$. In other words, $P_h^\pi(s, a)$ qualifies the visitation probability of state-action pair (s, a) at time step h . In this way, we get an equivalent dual form of the policy value [Puterman, 2014]:

$$V^\pi = \sum_{h=1}^H \sum_{(s,a) \in \mathcal{S} \times \mathcal{A}} P_h^\pi(s, a) r_h(s, a). \quad (2.1)$$

Imitation Learning. The goal of imitation learning is to learn a high quality policy without the reward function. To this end, we often assume there is a nearly optimal expert policy π^E that could interact with the environment and generate a dataset $\mathcal{D} = \{\mathbf{tr} = (s_1, a_1, s_2, a_2, \dots, s_H, a_H); s_1 \sim \rho, a_h \sim \pi_h^E(\cdot|s_h), s_{h+1} \sim P_h(\cdot|s_h, a_h), \forall h \in [H]\}$. Then, the learner can mimic the expert from expert dataset \mathcal{D} to obtain a high value policy. The quality of imitation is measured by the *policy value gap* [Abbeel and Ng, 2004, Ross and Bagnell, 2010, Rajaraman et al., 2020]: $V^{\pi^E} - V^\pi$. Following [Xu et al., 2020, Rajaraman et al., 2020], we assume the expert policy is deterministic.

Notation. We denote Π as the set of all deterministic policies for the learner. For a trajectory \mathbf{tr} in expert demonstrations \mathcal{D} , $\mathbf{tr}(s_h)$ and $\mathbf{tr}(s_h, a_h)$ denote the specific state and state-action pair at time step h in the trajectory \mathbf{tr} , respectively. Furthermore, $|\mathcal{D}|$ is the number of trajectories in \mathcal{D} . We write $a \gtrsim b$ if there exists a constant $C > 0$ such that $a \geq Cb$ by ignoring the lower order terms.

3 Transition-aware Adversarial Imitation Learning

In this section, we first focus on how to obtain a fine-grained estimator for AIL methods. Subsequently, we discuss the optimization issue in the related imitation learning problem. Finally, we give the statistical and computational guarantees of our transition-aware adversarial imitation algorithm.

3.1 Toward a Fine-grained Estimator

In this part, we consider the following imitation problem:

$$\min_{\pi \in \Pi} \frac{1}{H} \sum_{h=1}^H \left\| P_h^\pi(s, a) - P_h^{\pi^E}(s, a) \right\|_1. \quad (3.1)$$

This objective follows the principle of state-action distribution matching and is fundamental to AIL algorithms such as FEM [Abbeel and Ng, 2004], GTAL [Syed and Schapire, 2007] and GAIL [Ho and Ermon, 2016]. The main difference is that we aim to solve a ℓ_1 -norm based imitation learning problem in (3.1) while FEM, GTAL and GAIL aim to solve a ℓ_2 -norm, ℓ_∞ -norm and JS-divergence based imitation learning problems, respectively. Our first observation is that if (3.1) can be effectively solved, the induced policy value gap is small.

Lemma 3.1 (Error bound of AIL [Xu et al., 2020]). *Given an expert policy π^E , suppose that the policy π solves the IL problem in (3.1) to ε -optimal (i.e., $\frac{1}{H} \sum_{h=1}^H \left\| P_h^\pi(s, a) - P_h^{\pi^E}(s, a) \right\|_1 \leq \varepsilon$), then we have $V^{\pi^E} - V^\pi \leq H\varepsilon$.*

This lemma shows that there is no compounding error issue for state-action distribution matching. To solve (3.1) practically, we need to estimate $P_h^{\pi^E}$ with finite samples. A natural idea is to employ a maximum likelihood estimator [Abbeel and Ng, 2004, Syed and Schapire, 2007, Shani et al., 2021], which corresponds to “counting” under the tabular setting:

$$\left(\widehat{P}_h^{\pi^E} \circ \mathcal{D} \right) (s, a) := \frac{\sum_{\mathbf{tr} \in \mathcal{D}} \mathbb{I}\{\mathbf{tr}(s_h, a_h) = (s, a)\}}{|\mathcal{D}|}, \quad \forall h \in [H], (s, a) \in \mathcal{S} \times \mathcal{A}. \quad (3.2)$$

Remark 3.1. Unfortunately, we cannot prove that the imitation learning algorithm by solving (3.1) with the estimator in (3.2) could enjoy a better sample complexity compared with the simple algorithm BC. This is because to obtain an ε -optimal estimation (i.e., $\sum_{h=1}^H \|P_h^{\pi^E} - \hat{P}_h^{\pi^E}\|_1 \leq \varepsilon$), concentration inequality for the ℓ_1 -deviation [Weissman et al., 2003] implies that the required number of trajectories is at least of $\tilde{\mathcal{O}}(H^2|\mathcal{S}|/\varepsilon^2)$. This is unsatisfying since we know that the sample complexity of BC is already of $\tilde{\mathcal{O}}(H^2|\mathcal{S}|/\varepsilon)$ [Xu et al., 2020, Rajaraman et al., 2020]. A similar issue occurs in AIL methods such as FEM, GTAL and OAL that employ the maximum likelihood estimation in (3.2). Unfortunately, we validate that the upper bound on the sample complexity of AIL methods with (3.2) is tight by the numerical result shown in Figure 2b, which implies we have to improve AIL methods from an algorithmic perspective.

To tackle the sample efficiency issue of AIL, we propose a fine-grained estimator for $P_h^{\pi^E}$. First of all, let us introduce the notation \mathbf{tr}_h , which is the truncated trajectory up to time step h , i.e., $\mathbf{tr}_h = (s_1, a_1, \dots, s_h, a_h)$. Furthermore, define $\text{Tr}_h^{\pi^E}$ as the set of all truncated trajectories generated by π^E . Consequently, we can leverage the following decomposition for $P_h^{\pi^E}$:

$$P_h^{\pi^E}(s, a) = \sum_{\mathbf{tr}_h \in \text{Tr}_h^{\pi^E}} \mathbb{P}^{\pi^E}(\mathbf{tr}_h) \mathbb{I}\{\mathbf{tr}_h(s_h, a_h) = (s, a)\}, \quad (3.3)$$

where $\mathbb{P}^{\pi^E}(\mathbf{tr}_h)$ is the probability of the truncated trajectory \mathbf{tr}_h induced by the deterministic expert policy π^E . Note that $\mathbb{P}^{\pi^E}(\mathbf{tr}_h)$ can be computed if the transition function is known; specifically, $\mathbb{P}^{\pi^E}(\mathbf{tr}_h) = p(\mathbf{tr}(s_1)) \prod_{\ell=1}^{h-1} P_\ell(\mathbf{tr}(s_{\ell+1})|\mathbf{tr}(s_\ell), \mathbf{tr}(a_\ell))$.

To utilize (3.3), let us further introduce the notation $\text{Tr}_h^{\mathcal{D}} = \{\mathbf{tr}_h : \mathbf{tr}_h \in \mathcal{D}\}$; that is, $\text{Tr}_h^{\mathcal{D}}$ includes unique truncated trajectories in \mathcal{D} . Now, consider the dataset \mathcal{D} is randomly divided into two equal parts, i.e., $\mathcal{D} = \mathcal{D}_1 \cup \mathcal{D}_1^c$, then we have

$$\begin{aligned} P_h^{\pi^E}(s, a) &= \sum_{\mathbf{tr}_h \in \text{Tr}_h^{\mathcal{D}_1}} \mathbb{P}^{\pi^E}(\mathbf{tr}_h) \mathbb{I}\{\mathbf{tr}_h(s_h, a_h) = (s, a)\} \\ &\quad + \sum_{\mathbf{tr}_h \notin \text{Tr}_h^{\mathcal{D}_1}} \mathbb{P}^{\pi^E}(\mathbf{tr}_h) \mathbb{I}\{\mathbf{tr}_h(s_h, a_h) = (s, a)\}. \end{aligned}$$

Note that for $\mathbf{tr}_h \in \text{Tr}_h^{\mathcal{D}_1}$, all state-action pairs up to time step h are known from \mathcal{D}_1 . Therefore, we can compute the first term in the above decomposition exactly provided the transition is known. For the second term, we do not know some actions in $\mathbf{tr}_h \notin \text{Tr}_h^{\mathcal{D}_1}$ from \mathcal{D}_1 since \mathcal{D}_1 possibly does not contain every truncated trajectory visited by π^E . The good news is that we can leverage the complementary dataset \mathcal{D}_1^c to estimate such unknown actions. Concretely, we employ the mentioned maximum likelihood estimation for the second term on \mathcal{D}_1^c . By independence of trajectories, this is an unbiased estimation. In summary, we arrive at the following fine-grained estimation⁴:

$$\left(\tilde{P}_h^{\pi^E} \circ \mathcal{D} \right)(s, a) := \sum_{\mathbf{tr}_h \in \text{Tr}_h^{\mathcal{D}_1}} \mathbb{P}^{\pi^E}(\mathbf{tr}_h) \mathbb{I}\{\mathbf{tr}_h(s_h, a_h) = (s, a)\} + \left(\hat{P}_h^{\pi^E} \circ \mathcal{D}_1^c \right)(s, a), \quad (3.4)$$

where $\hat{P}_h^{\pi^E} \circ \mathcal{D}_1^c$ is based on the maximum likelihood estimation defined in (3.2). When there is no danger of confusion, we simply write $(\tilde{P}_h^{\pi^E} \circ \mathcal{D})(s, a)$ as $\tilde{P}_h^{\pi^E}(s, a)$. At a high level, the estimator in (3.4) utilizes the transition function information to obtain a more accurate estimation. Technically, we show that this estimator mainly corresponds to Bernoulli random variables estimation in high dimensional statistics. Importantly, the expectations of these Bernoulli random variables are well controlled so that Chernoff's bound could be applied to obtain a better sample complexity.

Lemma 3.2. Consider \mathcal{D} is randomly divided into two subsets, i.e., $\mathcal{D} = \mathcal{D}_1 \cup \mathcal{D}_1^c$ with $|\mathcal{D}_1| = |\mathcal{D}_1^c| = m/2$. Fix $\varepsilon \in (0, H)$ and $\delta \in (0, 1)$; suppose $H \geq 5$. If the number of trajectories in \mathcal{D} satisfies

$$m \gtrsim \frac{H^{3/2}|\mathcal{S}|}{\varepsilon} \log\left(\frac{H|\mathcal{S}|}{\delta}\right),$$

then with probability at least $1 - \delta$, we have $\sum_{h=1}^H \left\| \tilde{P}_h^{\pi^E}(s, a) - P_h^{\pi^E}(s, a) \right\|_1 \leq \varepsilon$.

Remark 3.2. This lemma indicates that the dependence of sample complexity on both H and ε is improved compared with the one of direct maximum likelihood estimation [Weissman et al., 2003]. Moreover, combined with Lemma 3.1, this suggests that the sample complexity of solving (3.1) with the estimator in (3.4) could be better than BC [Xu et al., 2020, Rajaraman et al., 2020], FEM [Abbeel and Ng, 2004], GTAL [Syed and Schapire, 2007] and OAL [Shani et al., 2021] in the worst-case.

⁴To help readers understand this estimator, we provide a detailed example in Appendix C.

Remark 3.3. The proposed estimator is inspired by the coupling analysis in [Rajaraman et al., 2020]. However, Rajaraman et al. [2020] did not explicitly report any practical estimator for $P_h^{\pi^E}$ as they conjectured “the conventional minimum distance functional (AIL) approach, \dots , does not achieve the rate”. Nevertheless, we provide a positive answer that the “conventional minimum distance functional (AIL)” with (3.4) could achieve the same sample complexity as MIMIC-MD [Rajaraman et al., 2020] as shown in Theorem 3.1.

3.2 Algorithm Implementation

We now consider the optimization issue of (3.1). Our first observation is that (3.1) cannot be exactly solved in polynomial time. Luckily, we could solve it approximately and the final sample complexity does not change too much. In particular, we utilize the dual representation of ℓ_1 -norm and the minimax theorem [Bertsekas, 2016], and transform (3.1) into the following minimax optimization problem:

$$\max_{w \in \mathcal{W}} \min_{\pi \in \Pi} \sum_{h=1}^H \sum_{(s,a) \in \mathcal{S} \times \mathcal{A}} w_h(s,a) \left(\tilde{P}_h^{\pi^E}(s,a) - P_h^{\pi}(s,a) \right). \quad (3.5)$$

where $\mathcal{W} = \{w : \|w\|_\infty \leq 1\}$ is the unit ball. We see that the inner problem in (3.5) is to maximize the policy value of π given the reward function $w_h(s,a)$ (see (2.1) for the dual form of policy value). For the outer optimization problem, we can use online gradient descent methods [Shalev-Shwartz, 2012] so that the overall objective can finally reach an approximate saddle point. Formally, let us define the objective

$$f^{(t)}(w) := \sum_{h=1}^H \sum_{(s,a) \in \mathcal{S} \times \mathcal{A}} w_h(s,a) \left(P_h^{\pi^{(t)}}(s,a) - \tilde{P}_h^{\pi^E}(s,a) \right), \quad (3.6)$$

where $\pi^{(t)}$ is the optimized policy π at iteration t . Then the update rule for w is:

$$w^{(t+1)} := \mathcal{P}_{\mathcal{W}} \left(w^{(t)} - \eta^{(t)} \nabla f^{(t)}(w^{(t)}) \right),$$

where $\eta^{(t)} > 0$ is the stepsize to be chosen later, and $\mathcal{P}_{\mathcal{W}}$ is the Euclidean projection on the unit ball \mathcal{W} , i.e., $\mathcal{P}_{\mathcal{W}}(w) := \operatorname{argmin}_{z \in \mathcal{W}} \|z - w\|_2$. The procedure of solving (3.5) is outlined in Algorithm 1.

Algorithm 1 Transition-aware Adversarial Imitation Learning (TAIL)

Input: expert demonstrations \mathcal{D} , number of iterations T , step size $\eta^{(t)}$, and initialization $w^{(1)}$.

- 1: Randomly split \mathcal{D} into two equal parts: $\mathcal{D} = \mathcal{D}_1 \cup \mathcal{D}_1^c$ and obtain the estimation $\tilde{P}_h^{\pi^E}$ in (3.4).
- 2: **for** $t = 1, 2, \dots, T$ **do**
- 3: $\pi^{(t)} \leftarrow$ solve the optimal policy with the reward function $w^{(t)}$ up to an error of ε_{opt} .
- 4: Compute the state-action distribution $P_h^{\pi^{(t)}}$ for $\pi^{(t)}$.
- 5: Update $w^{(t+1)} := \mathcal{P}_{\mathcal{W}} \left(w^{(t)} - \eta^{(t)} \nabla f^{(t)}(w^{(t)}) \right)$ with $f^{(t)}(w)$ defined in (3.6).
- 6: **end for**
- 7: Compute the mean state-action distribution $\bar{P}_h(s,a) = \sum_{t=1}^T P_h^{\pi^{(t)}}(s,a)/T$.
- 8: Derive $\bar{\pi}_h(a|s) \leftarrow \bar{P}_h(s,a) / \sum_a \bar{P}_h(s,a)$.

Output: policy $\bar{\pi}$.

Now we present our theoretical result on the sample complexity of TAIL.

Theorem 3.1. Fix $\varepsilon \in (0, H)$ and $\delta \in (0, 1)$; suppose $H \geq 5$. Consider the approach TAIL displayed in Algorithm 1 and $\bar{\pi}$ is output policy, assume that the optimization error $\varepsilon_{\text{opt}} \leq \varepsilon/2$, if the number of expert demonstrations, the number of iterations T and the step size $\eta^{(t)}$ satisfy

$$m \gtrsim \frac{H^{3/2}|\mathcal{S}|}{\varepsilon} \log \left(\frac{H|\mathcal{S}|}{\delta} \right), \quad T \gtrsim \frac{H^2|\mathcal{S}||\mathcal{A}|}{\varepsilon^2}, \quad \eta^{(t)} := \sqrt{\frac{|\mathcal{S}||\mathcal{A}|}{8T}}.$$

Then with probability at least $1 - \delta$, we have $V^{\pi^E} - V^{\bar{\pi}} \leq \varepsilon$.

Remark 3.4. The optimization problem corresponding to line 3 of Algorithm 1 can be solved efficiently to an acceptable error by value iteration [Puterman, 2014] or policy gradient based methods [Agarwal et al., 2020].

Remark 3.5. We see that the sample complexity of the proposed approach matches the lower bound of $\tilde{\Omega}(H^{3/2}|\mathcal{S}|/\varepsilon)$ [Rajaraman et al., 2021] up to a logarithmic term. This implies that Algorithm 1 is nearly minimax optimal under the known transition setting. The tightness of sample complexity in Theorem 3.1 is empirically verified in Appendix G.

4 When the Transition Is Unknown

In this part, we consider a common setting where the learner does not know the exact transition function but can interact with the environment. Under the unknown transition setting, we focus on both the number of expert demonstrations and the number of environment interactions (i.e., the trajectories collected by the learner). Here we refer to the above two measures as *expert sample complexity* and *interaction complexity*, respectively. In Algorithm 1, there are three steps requiring the knowledge of transition functions: **1**) establish the fine-grained estimator, **2**) learn the optimal policy with the inferred reward function and **3**) compute the state-action distribution of the learner's policy. In the following, we show how to address these issues under the unknown transition setting.

For the first point, recall that the computation of $\sum_{\mathbf{tr}_h \in \text{Tr}_h^{\mathcal{D}_1}} \mathbb{P}^{\pi^E}(\mathbf{tr}_h) \mathbb{I}\{\mathbf{tr}_h(s_h, a_h) = (s, a)\}$ in (3.4) relies on the transition function. Under the unknown transition setting, we may estimate this term with new trajectories collected from the environment. We present a key observation as follows.

Lemma 4.1. *We define $\Pi(\mathcal{D}_1)$ as the set of policies, each of which takes expert action on states contained in \mathcal{D}_1 . For each $\pi \in \Pi(\mathcal{D}_1)$, $\forall h \in [H]$ and $(s, a) \in \mathcal{S} \times \mathcal{A}$, we have*

$$\sum_{\mathbf{tr}_h \in \text{Tr}_h^{\mathcal{D}_1}} \mathbb{P}^{\pi^E}(\mathbf{tr}_h) \mathbb{I}\{\mathbf{tr}_h(s_h, a_h) = (s, a)\} = \sum_{\mathbf{tr}_h \in \text{Tr}_h^{\mathcal{D}_1}} \mathbb{P}^{\pi}(\mathbf{tr}_h) \mathbb{I}\{\mathbf{tr}_h(s_h, a_h) = (s, a)\}.$$

Note that $\Pi(\mathcal{D}_1)$ is the set of policies obtained by BC. Intuitively, on states along trajectory $\mathbf{tr}_h \in \text{Tr}_h^{\mathcal{D}_1}$, a policy $\pi \in \Pi(\mathcal{D}_1)$ exactly takes the expert action. Therefore, the trajectory probabilities induced by π and π^E are equal up to time step h . With this lemma, we can roll out the policy $\pi \in \Pi(\mathcal{D}_1)$ to collect trajectories and to establish an unbiased estimator. Concretely, we first learn a policy $\pi \in \Pi(\mathcal{D}_1)$ by BC, and then roll out π to collect a new dataset \mathcal{D}' . The new estimator is formulated as

$$(\tilde{P}_h^{\pi^E} \circ \mathcal{D})(s, a) := (\hat{P}_h^{\pi^E} \circ \mathcal{D}')(s, a) + (\hat{P}_h^{\pi^E} \circ \mathcal{D}_1^c)(s, a), \quad (4.1)$$

where $(\hat{P}_h^{\pi^E} \circ \mathcal{D}')(s, a) = \sum_{\mathbf{tr}_h \in \mathcal{D}'} \mathbb{I}\{\mathbf{tr}_h(s_h, a_h) = (s, a), \mathbf{tr}_h \in \text{Tr}_h^{\mathcal{D}_1}\} / |\mathcal{D}'|$. The expert sample complexity and interaction complexity of (4.1) are given in Lemma E.1 in Appendix E.2. Importantly, this alternative estimator does not undermine expert sample complexity and interaction complexity.

To deal with the second and third points, we consider a model-based approach [Sutton and Barto, 2018]. In particular, we first employ some exploratory policies to collect n' trajectories in the environment, and then build an empirical transition model from n' new trajectories by “counting”; $\hat{P}_h(s'|s, a) = n_h(s, a, s') / n_h(s, a)$, where $n_h(s, a, s')$ and $n_h(s, a)$ denote the visitation number of (s, a, s') and (s, a) at time step h in n' new trajectories, respectively. Once this empirical model is built, policy optimization and state-action distribution estimation can be implemented without further interaction. As shown in Algorithm 1, AIL needs to perform policy optimization with different inferred rewards and hence, a reward-free method named RF-Express [Ménard et al., 2020] is applied to collect trajectories to build the empirical transition model. We name this model-based AIL algorithm as MB-TAIL. The overall procedure of MB-TAIL under the unknown transition setting is outlined in Algorithm 2.

Theorem 4.1. *Fix $\varepsilon \in (0, 1)$ and $\delta \in (0, 1)$; suppose $H \geq 5$. Under the unknown transition setting, consider MB-TAIL displayed in Algorithm 2 and $\bar{\pi}$ is output policy, assume that the optimization error $\varepsilon_{\text{opt}} \leq \varepsilon/2$, the number of iterations and the step size are the same as in Theorem 3.1, if the expert sample complexity and the total interaction complexity satisfy*

$$m \gtrsim \frac{H^{3/2}|\mathcal{S}|}{\varepsilon} \log\left(\frac{H|\mathcal{S}|}{\delta}\right), n \gtrsim \frac{H^2|\mathcal{S}|}{\varepsilon^2} \log\left(\frac{H|\mathcal{S}|}{\delta}\right), n' \gtrsim \frac{H^3|\mathcal{S}||\mathcal{A}|}{\varepsilon^2} \left(|\mathcal{S}| + \log\left(\frac{H|\mathcal{S}||\mathcal{A}|}{\delta\varepsilon}\right)\right)$$

Then with probability at least $1 - \delta$, we have $V^{\pi^E} - V^{\bar{\pi}} \leq \varepsilon$.

Remark 4.1. *Under the unknown transition setting, the expert sample complexity of MB-TAIL is still of $\tilde{\mathcal{O}}(H^{3/2}|\mathcal{S}|/\varepsilon)$. This implies that even when the transition function is unknown but interaction is allowed, MB-TAIL is still nearly minimax optimal with respect to the expert sample complexity.*

Remark 4.2. *The total interaction complexity of MB-TAIL is of $\tilde{\mathcal{O}}(H^3|\mathcal{S}|^2|\mathcal{A}|/\varepsilon^2)$, which is an improvement over the best known result of $\tilde{\mathcal{O}}(H^4|\mathcal{S}|^2|\mathcal{A}|/\varepsilon^2)$ in [Shani et al., 2021]. This is partially because the reward-free exploration methods are more efficient in adversarial imitation learning where the inferred reward function varies over iterations.*

Remark 4.3. *Seminal works of Abbeel and Ng [2005], Syed and Schapire [2007] also considered the unknown transition setting, but they used expert demonstrations to learn an empirical transition function. Accordingly, the expert sample complexities of their algorithms are huge as shown in Table 1. Therefore, algorithms in Abbeel and Ng [2005], Syed and Schapire [2007] are impractical in the sense that if the number of expert demonstrations is large enough to obtain an accurate empirical transition function, the simple algorithm BC could perform well.*

Algorithm 2 Model-based Transition-aware Adversarial Imitation Learning (MB-TAIL)

Input: expert demonstrations \mathcal{D} , number of iterations T , step size $\eta^{(t)}$, and initialization $w^{(1)}$.

- 1: Randomly split \mathcal{D} into two equal parts: $\mathcal{D} = \mathcal{D}_1 \cup \mathcal{D}_1^c$.
- 2: Learn $\pi \in \Pi(\mathcal{D}_1)$ by BC and roll out π to obtain dataset \mathcal{D}' with $|\mathcal{D}'| = n$.
- 3: Obtain the estimation $\tilde{P}_h^{\pi^E}$ in (4.1) with $\mathcal{D} = \mathcal{D}_1 \cup \mathcal{D}_1^c$ and \mathcal{D}' .
- 4: Invoke RF-Express to collect n' trajectories and learn an empirical transition function $\hat{\mathcal{P}}$.
- 5: **for** $t = 1, 2, \dots, T$ **do**
- 6: $\pi^{(t)} \leftarrow$ solve the optimal policy with the reward function $w^{(t)}$ and the learned transition function $\hat{\mathcal{P}}$ up to an error of ε_{opt} .
- 7: Compute the state-action distribution $\ddot{P}_h^{\pi^{(t)}}$ for $\pi^{(t)}$ with the learned transition function $\hat{\mathcal{P}}$.
- 8: Update $w^{(t+1)} := \mathcal{P}_{\mathcal{W}}(w^{(t)} - \eta^{(t)} \nabla f^{(t)}(w^{(t)}))$ with $f^{(t)}(w)$ defined in (3.6).
- 9: **end for**
- 10: Compute the mean state-action distribution $\bar{P}_h(s, a) = \sum_{t=1}^T \ddot{P}_h^{\pi^{(t)}}(s, a)/T$.
- 11: Derive $\bar{\pi}_h(a|s) \leftarrow \bar{P}_h(s, a) / \sum_a \bar{P}_h(s, a)$.

Output: policy $\bar{\pi}$.

5 Case Studies

In this section, we conduct experiments to validate the sample and interaction efficiency of the proposed algorithms. We focus on two MDPs: *Reset Cliff* and *Standard Imitation* shown in Figure 1, which are adapted from [Rajaraman et al., 2020]. Experiment details are given in Appendix F.

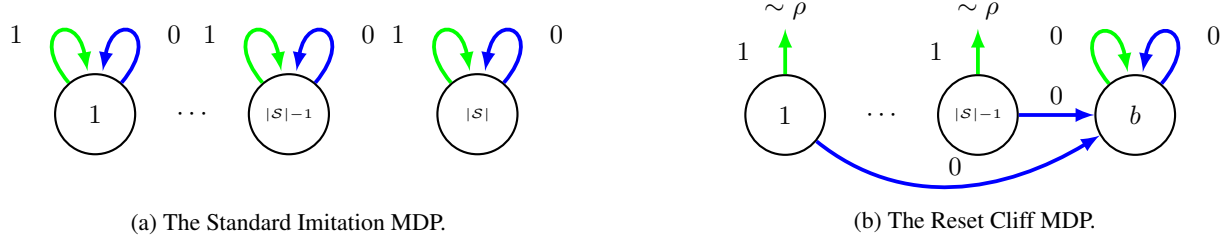


Figure 1: Two MDPs [Rajaraman et al., 2020] used for comparison. Green and blue arrows indicate state transitions under the expert and non-expert actions, respectively. Digits on arrows mean reward values.

5.1 Known Transition Setting

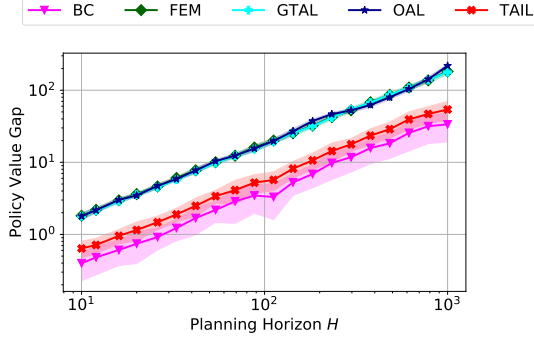
We first consider the known transition setting with methods⁵ including BC [Pomerleau, 1991], FEM [Abbeel and Ng, 2004], GTAL [Syed and Schapire, 2007], OAL [Shani et al., 2021] and TAIL (see Algorithm 1). We aim to study the dependence on H and ε appeared in the sample complexity. In this part, figures use logarithmic scales such that we can read the order dependence from slopes of curves. Specifically, a worst-case sample complexity $m \gtrsim H^\alpha |\mathcal{S}| / \varepsilon^\beta$ implies the policy value gap $V^{\pi^E} - V^\pi \lesssim H^{\alpha/\beta} |\mathcal{S}|^{1/\beta} / m^{1/\beta}$. Then, we see that

$$\log(V^{\pi^E} - V^\pi) \lesssim (\alpha/\beta) \log(H) - 1/\beta \log(m) + 1/\beta \log(|\mathcal{S}|).$$

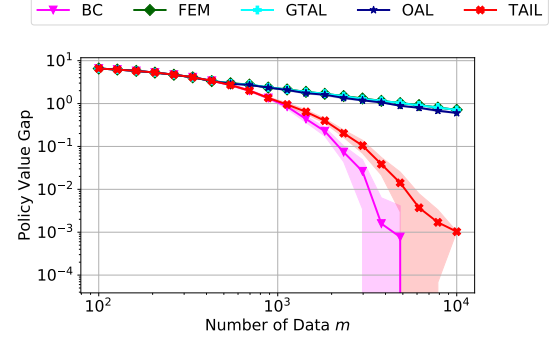
For example, the sample complexity $\tilde{\mathcal{O}}(H^2 |\mathcal{S}| / \varepsilon^2)$ of FEM would hint slope 1 w.r.t $\log(H)$ and slope $-1/2$ w.r.t $\log(m)$ for its log policy value gap; the sample complexity $\tilde{\mathcal{O}}(H^{3/2} |\mathcal{S}| / \varepsilon)$ of TAIL similarly suggests slope $3/2$ w.r.t $\log(H)$ and slope -1 w.r.t. $\log(m)$ for its log policy value gap. It is worth mentioning that these implications are true only on “hard” instances.

Case Study on Standard Imitation. Under Standard Imitation, each state is absorbing and the agent gets +1 reward only by taking expert action (shown in green). Different from [Rajaraman et al., 2020], the initial state distribution ρ is $(\frac{1}{|\mathcal{S}|}, \dots, \frac{1}{|\mathcal{S}|})$ to better study the sample complexity of AIL methods.

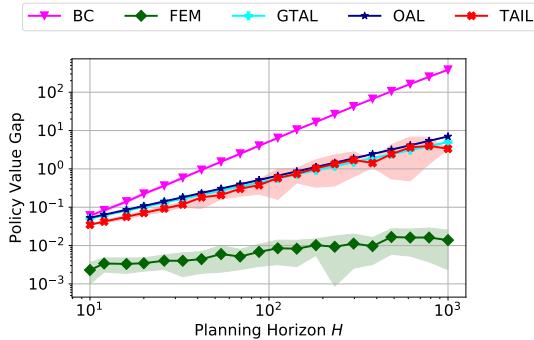
⁵MIMIC-MD runs out of memory on the machine with 128 GB RAM when solving IL tasks with planning horizons that exceed 100. Thus we do not involve MIMIC-MD for comparison.



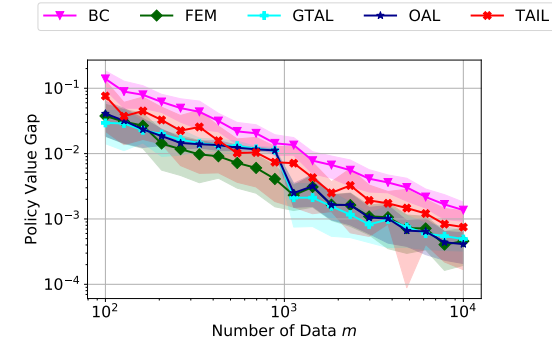
(a) On the planning horizon in Standard Imitation.



(b) On the expert sample size in Standard Imitation.



(c) On the planning horizon in Reset Cliff.



(d) On the expert sample size in Reset Cliff.

Figure 2: The policy value gap (i.e., $V^{\pi^E} - V^\pi$) in Standard Imitation and Reset Cliff. The solid lines are mean of results and the shaded region corresponds to the standard deviation over 20 random seeds (same with the following figure).

Firstly, we focus on the planning horizon dependence issue; see the result in Figure 2a. In particular, the numerical result shows that the policy value gap of all methods grows linearly with the planning horizon. This is reasonable since each state in Standard Imitation is absorbing; consequently, there is no compounding error issue. Notice that Standard Imitation is not the worst-case MDP for BC due to its absorbing structure. However, Standard Imitation is still challenging for existing AIL approaches (FEM, GTAL, and OAL) and thus can be used to validate the tightness of their sample complexities listed in Table 1 as we illustrate in the following.

Secondly, we display the result regarding the number of expert demonstrations in Figure 2b. Under Standard Imitation, the state distribution of every policy is a uniform distribution at every time step, which raises a statistical estimation challenge for AIL. From Figure 2b, we clearly see that the slopes of FEM, GTAL and OAL w.r.t $\log(m)$ are around $-1/2$. This can be explained by their sample complexity $\tilde{O}(H^2|\mathcal{S}|/\varepsilon)$, which implies $\log(V^{\pi^E} - V^\pi) \lesssim -1/2 \log(m) + \text{constant}$. Though it is theoretically challenging to claim that existing AIL methods analysis is tight by providing a lower bound, we believe that this claim is true from results in Figure 2a and 2b. As for our method, as shown in Figure 2b, the policy value gap of TAIL diminishes substantially faster than FEM, GTAL and OAL, which verifies the sample efficiency of TAIL. The fast diminishing rate of BC is due to the quick concentration rate of missing mass [McAllester and Ortiz, 2003]; see [Rajaraman et al., 2020] for more explanation.

Case Study on Reset Cliff. Under the Reset Cliff, the agent gets $+1$ reward by taking the expert action (shown in green) on states except the bad state b , then the next state is renewed according to ρ ; once taking a non-expert action (shown in blue), the agent goes to the absorbing state b and always gets 0 reward. The initial state distribution ρ is $(\frac{1}{m+1}, \dots, \frac{1}{m+1}, 1 - \frac{|\mathcal{S}|-2}{m+1}, 0)$ as suggested in [Rajaraman et al., 2020].

On the one hand, Reset Cliff highlights the compounding error issue and the numerical result about the planning horizon is given in Figure 2c. In particular, on states uncovered in expert demonstrations, BC randomly selects an action. It is very likely that the agent picks up a non-expert action, goes to the bad state, and gets 0 reward in the remaining time.

In contrast, AIL can avoid this issue via imitating expert state-action distribution. To see this, consider a good state (e.g., state 1) at time step h appears in the dataset, the agent must follow the expert actions at all time steps before h ; otherwise, the agent will go to the bad state and cannot visit the observed good state at time step h , which violates the state-action distribution matching principle. As such, we expect the slopes of BC of AIL w.r.t. $\log(H)$ are 2 and 1, respectively. This argument is verified by the result in Figure 2c.

On the other hand, we consider the dependence on the number of expert demonstrations; the corresponding numerical result is shown in Figure 2d. From Figure 2d, we see that the slopes of all methods are around -1 . Combined with the quadratic horizon dependency of BC, we empirically validate that the sample complexity analysis of BC is tight. Note that Reset Cliff is not the worst-case MDP for AIL approaches (FEM, GTAL, and OAL) as we have analyzed, thus AIL approaches indeed have better performance on Reset Cliff compared with the worst-case performance listed in Table 1.

5.2 Unknown Transition Setting

In this part, we study the interaction complexity under the unknown transition setting. We still use the above two MDPs, but they may not be hard instances; so we do not verify the tightness of order dependency. The comparison methods involve BC [Pomerleau, 1991], OAL [Shani et al., 2021] and MB-TAIL (see Algorithm 2). All algorithms are provided with the same expert demonstrations.

Empirical results are displayed in Figure 3. Note that BC does not need interaction in principle. Similar to the results shown in Figure 2, BC performs worse than AIL methods on Reset Cliff while BC could be better than AIL on Standard Imitation. Moreover, we see that MB-TAIL substantially outperforms OAL provided with the same number of environment interactions. This is partially because MB-TAIL builds the empirical model in a reward-free fashion, which is more efficient than the online learning approach in OAL.



(a) On the number of interactions in Standard Imitation.

(b) On the number of interactions in Reset Cliff.

Figure 3: The policy value gap (i.e., $V^{\pi^E} - V^{\pi}$) in Standard Imitation and Reset Cliff.

6 Conclusion

This paper is motivated by the sample efficiency issue of previous AIL algorithms. To deal with this issue, we develop a new AIL approach that enjoys an improved sample complexity of $\tilde{\mathcal{O}}(H^{3/2}|\mathcal{S}|/\varepsilon)$, which is nearly minimax optimal. Finally, we develop a model-based AIL approach with an improved interaction complexity of $\tilde{\mathcal{O}}(H^3|\mathcal{S}|^2|\mathcal{A}|/\varepsilon^2)$ under the unknown transition setting. An important question we raise is whether we can incorporate more efficient exploration methods to further reduce the interaction complexity of AIL approaches.

References

- P. Abbeel and A. Y. Ng. Apprenticeship learning via inverse reinforcement learning. In *Proceedings of the 21st International Conference on Machine Learning*, pages 1–8, 2004.
- P. Abbeel and A. Y. Ng. Exploration and apprenticeship learning in reinforcement learning. In *Proceedings of the 22nd International Conference on Machine Learning*, pages 1–8, 2005.
- A. Agarwal, S. M. Kakade, J. D. Lee, and G. Mahajan. Optimality and approximation with policy gradient methods in markov decision processes. In *Proceedings of the 33rd Annual Conference on Learning Theory*, pages 64–66, 2020.
- A. Beck and M. Teboulle. Mirror descent and nonlinear projected subgradient methods for convex optimization. *Operation Research Letters*, 31(3):167–175, 2003.

D. P. Bertsekas. *Nonlinear Programming*. Athena Scientific, 2016.

K. Brantley, W. Sun, and M. Henaff. Disagreement-regularized imitation learning. In *Proceedings of the 8th International Conference on Learning Representations*, 2020.

K. Chang, A. Krishnamurthy, A. Agarwal, H. D. III, and J. Langford. Learning to search better than your teacher. In *Proceedings of the 32nd International Conference on Machine Learning*, pages 2058–2066, 2015.

X. Chen, S. Li, H. Li, S. Jiang, Y. Qi, and L. Song. Generative adversarial user model for reinforcement learning based recommendation system. In *Proceedings of the 36th International Conference on Machine Learning*, pages 1052–1061, 2019.

H. Daumé, J. Langford, and D. Marcu. Search-based structured prediction. *Machine Learning*, 75(3):297–325, 2009.

C. Finn, S. Levine, and P. Abbeel. Guided cost learning: deep inverse optimal control via policy optimization. In *Proceedings of the 33rd International Conference on Machine Learning*, pages 49–58, 2016.

M. Frank, P. Wolfe, et al. An algorithm for quadratic programming. *Naval research logistics quarterly*, 3(1-2):95–110, 1956.

J. Fu, K. Luo, and S. Levine. Learning robust rewards with adversarial inverse reinforcement learning. In *Proceedings of the 6th International Conference on Learning Representations*, 2018.

J. Ho and S. Ermon. Generative adversarial imitation learning. In *Advances in Neural Information Processing Systems 29*, pages 4565–4573, 2016.

C. Jin, Z. Allen-Zhu, S. Bubeck, and M. I. Jordan. Is q-learning provably efficient? In *Advances in Neural Information Processing Systems 30*, pages 4868–4878, 2018.

L. Ke, M. Barnes, W. Sun, G. Lee, S. Choudhury, and S. S. Srinivasa. Imitation learning as f-divergence minimization. *arXiv*, 1905.12888, 2019.

I. Kostrikov, K. K. Agrawal, D. Dwibedi, S. Levine, and J. Tompson. Discriminator-actor-critic: Addressing sample inefficiency and reward bias in adversarial imitation learning. In *Proceedings of the 7th International Conference on Learning Representations*, 2019.

I. Kostrikov, O. Nachum, and J. Tompson. Imitation learning via off-policy distribution matching. In *Proceedings of the 8th International Conference on Learning Representations*, 2020.

Y. T. Lee and A. Sidford. Efficient inverse maintenance and faster algorithms for linear programming. In *Proceedings of IEEE 56th Annual Symposium on Foundations of Computer Science*, pages 230–249, 2015.

S. Levine, C. Finn, T. Darrell, and P. Abbeel. End-to-end training of deep visuomotor policies. *Journal of Machine Learning Research*, 17(39):1–40, 2016.

T. P. Lillicrap, J. J. Hunt, A. Pritzel, N. Heess, T. Erez, Y. Tassa, D. Silver, and D. Wierstra. Continuous control with deep reinforcement learning. In *Proceedings of the 4th International Conference on Learning Representations*, 2016.

D. A. McAllester and L. E. Ortiz. Concentration inequalities for the missing mass and for histogram rule error. *Journal of Machine Learning Research*, 4:895–911, 2003.

P. Ménard, O. D. Domingues, A. Jonsson, E. Kaufmann, E. Leurent, and M. Valko. Fast active learning for pure exploration in reinforcement learning. *arXiv*, 2007.13442, 2020.

V. Mnih, K. Kavukcuoglu, D. Silver, A. A. Rusu, J. Veness, M. G. Bellemare, A. Graves, M. Riedmiller, A. K. Fidjeland, G. Ostrovski, et al. Human-level control through deep reinforcement learning. *nature*, 518(7540):529–533, 2015.

F. Orabona. A modern introduction to online learning. *arXiv*, 1912.13213, 2019.

D. Pomerleau. Efficient training of artificial neural networks for autonomous navigation. *Neural Computation*, 3(1): 88–97, 1991.

M. L. Puterman. *Markov Decision Processes: Discrete Stochastic Dynamic Programming*. John Wiley & Sons, 2014.

N. Rajaraman, L. F. Yang, J. Jiao, and K. Ramchandran. Toward the fundamental limits of imitation learning. In *Advances in Neural Information Processing Systems 33*, pages 2914–2924, 2020.

N. Rajaraman, Y. Han, L. F. Yang, K. Ramchandran, and J. Jiao. Provably breaking the quadratic error compounding barrier in imitation learning, optimally. *arXiv*, 2102.12948, 2021.

S. Ross and D. Bagnell. Efficient reductions for imitation learning. In *Proceedings of the 13rd International Conference on Artificial Intelligence and Statistics*, pages 661–668, 2010.

S. Ross, G. J. Gordon, and D. Bagnell. A reduction of imitation learning and structured prediction to no-regret online learning. In *Proceedings of the 14th International Conference on Artificial Intelligence and Statistics*, pages 627–635, 2011.

S. Shalev-Shwartz. Online learning and online convex optimization. *Foundations and Trends in Machine Learning*, 4 (2):107–194, 2012.

L. Shani, T. Zahavy, and S. Mannor. Online apprenticeship learning. *arXiv*, 2102.06924, 2021.

J. Shi, Y. Yu, Q. Da, S. Chen, and A. Zeng. Virtual-taobao: virtualizing real-world online retail environment for reinforcement learning. In *Proceedings of the 33rd AAAI Conference on Artificial Intelligence*, pages 4902–4909, 2019.

D. Silver, A. Huang, C. J. Maddison, A. Guez, L. Sifre, G. Van Den Driessche, J. Schrittwieser, I. Antonoglou, V. Panneershelvam, M. Lanctot, et al. Mastering the game of go with deep neural networks and tree search. *nature*, 529(7587):484–489, 2016.

R. S. Sutton and A. G. Barto. *Reinforcement Learning: An Introduction*. MIT press, 2018.

U. Syed and R. E. Schapire. A game-theoretic approach to apprenticeship learning. In *Advances in Neural Information Processing Systems 20*, pages 1449–1456, 2007.

F. Torabi, G. Warnell, and P. Stone. Behavioral cloning from observation. In *Proceedings of the 27th International Joint Conference on Artificial Intelligence*, pages 4950–4957, 2018.

R. Vershynin. *High-Dimensional Probability: An Introduction with Applications in Data Science*. Cambridge University Press, 2018.

Y. Wang, T. Liu, Z. Yang, X. Li, Z. Wang, and T. Zhao. On computation and generalization of generative adversarial imitation learning. In *Proceedings of the 8th International Conference on Learning Representations*, 2020.

T. Weissman, E. Ordentlich, G. Seroussi, S. Verdu, and M. J. Weinberger. Inequalities for the l_1 deviation of the empirical distribution. *Hewlett-Packard Labs, Technical Report*, 2003.

T. Xu, Z. Li, and Y. Yu. Error bounds of imitating policies and environments. In *Advances in Neural Information Processing Systems 33*, pages 15737–15749, 2020.

T. Zahavy, A. Cohen, H. Kaplan, and Y. Mansour. Apprenticeship learning via frank-wolfe. In *Proceedings of the 34th AAAI Conference on Artificial Intelligence*, pages 6720–6728, 2020.

A Notation

Table 2: Notations

Symbol	Meaning
\mathcal{S}	the state space
\mathcal{A}	the action space
$\mathcal{P} = \{P_1, \dots, P_H\}$	the transition function
H	the horizon
ρ	the initial state distribution
$r = \{r_1, \dots, r_H\}$	the reward function
$\pi = \{\pi_1, \dots, \pi_h\}$	non-stationary policy
π^E	the expert policy
V^π	policy value
ε	the policy value gap
δ	failure probability
$P_h^\pi(s)$	state distribution
$P_h^\pi(s, a)$	state-action distribution
$\text{tr} = (s_1, a_1, \dots, s_H, a_H)$	the trajectory
$\text{tr}_h = (s_1, a_1, \dots, s_h, a_h)$	the truncated trajectory
$\text{tr}(s_h)$	the state at time step h in tr
$\text{tr}(a_h)$	the action at time step h in tr
$\text{tr}(s_h, a_h)$	the state-action pair at time step h in tr
\mathcal{D}	expert demonstrations
m	number of expert demonstrations
$\left(\hat{P}_h^{\pi^E} \circ \mathcal{D}\right)(s, a)$	maximum likelihood estimator in \mathcal{D}
$\left(\tilde{P}_h^{\pi^E} \circ \mathcal{D}\right)(s, a)$	fine-grained estimator in \mathcal{D}
$\mathbb{P}^{\pi^E}(\text{tr})$	probability of the trajectory tr under the expert policy π^E
$\mathbb{P}^{\pi^E}(\text{tr}_h)$	probability of the truncated trajectory tr_h under the expert policy π^E
$\text{Tr}_h^{\mathcal{D}}$	the set of trajectories, each of which
	matches certain trajectory in \mathcal{D} up to time step h
$\pi^{(t)}$	the policy obtained in the iteration t
$w^{(t)}$	the reward function learned in the iteration t
$\eta^{(t)}$	the step size in the iteration t
$f^{(t)}(w)$	the objective function in the iteration t
$\bar{P}_h(s, a)$	the mean state-action distribution
$\bar{\pi}$	the policy derived by the mean state-action distribution
$\Pi(\mathcal{D}_1)$	the set of policies which take the expert action on states covered in \mathcal{D}_1
$\hat{\mathcal{P}}$	the empirical transition function
$\hat{P}_h^\pi(s, a)$	the state-action distribution of π under the empirical transition function $\hat{\mathcal{P}}$

B From Regret Guarantee to PAC Guarantee

In [Shani et al., 2021], authors proved a regret guarantee for their OAL algorithm. In particular, Shani et al. [2021] showed that with a high probability $1 - \delta'$, we have

$$\sum_{k=1}^K V^{\pi^E} - V^{\pi_k} \leq \tilde{\mathcal{O}} \left(\sqrt{H^4 |\mathcal{S}|^2 |\mathcal{A}| K} + \sqrt{H^3 |\mathcal{S}| |\mathcal{A}| K^2 / m} \right), \quad (\text{B.1})$$

where π^k is the policy obtained at episode k , K is the number of interaction episodes, and m is the number of expert trajectories. First of all, the second term in (B.1) that involves the statistical estimation error about the expert policy reduces to $\tilde{\mathcal{O}}(\sqrt{H^2 |\mathcal{S}| K^2 / m})$ under the assumption that the expert policy is deterministic.

To further convert this regret guarantee to the PAC guarantee considered in this paper, we can apply Markov's inequality as suggested by [Jin et al., 2018]. Concretely, let $\bar{\pi}$ be the policy that randomly chosen from $\{\pi^1, \pi^2, \dots, \pi^K\}$ with equal probability, then we have

$$\mathbb{P} \left(V^{\pi^E} - V^{\bar{\pi}} \geq \varepsilon \right) \leq \frac{1}{\varepsilon} \mathbb{E} \left[\frac{1}{K} \sum_{k=1}^K V^{\pi^E} - V^{\pi_k} \right] \leq \frac{1}{\varepsilon} \left(\tilde{\mathcal{O}} \left(\sqrt{\frac{H^4 |\mathcal{S}|^2 |\mathcal{A}|}{K}} + \sqrt{H^2 |\mathcal{S}| / m} \right) + \delta' H \right),$$

Therefore, if we set $\delta' = \varepsilon \delta / (3H)$, and

$$K = \tilde{\mathcal{O}} \left(\frac{H^4 |\mathcal{S}|^2 |\mathcal{A}|}{\varepsilon^2 \delta^2} \right), \quad m = \tilde{\mathcal{O}} \left(\frac{H^2 |\mathcal{S}|}{\varepsilon^2} \right),$$

we obtain that $\mathbb{P}(V^{\pi^E} - V^{\bar{\pi}} \geq \varepsilon) \leq \delta$. As commented in [Ménard et al., 2020], this transformation leads to a worse dependence on failure probability δ , but the sample complexity dependence on other terms does not change.

C An Illustrating Example

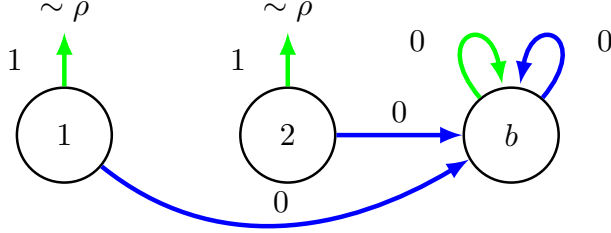


Figure 4: The Reset Cliff MDP with three states. There are two actions, shown in green and blue. The expert policy always takes the green action. The initial state distribution is $\rho = (\rho(\textcircled{1}), \rho(\textcircled{2}), \rho(\textcircled{b})) = (\frac{1}{100}, \frac{99}{100}, 0)$. At any state except the bad state b , if the agent plays the same action as the expert does, the agent is renewed according to ρ . Otherwise, the agent goes to the bad state b .

Here we provide an example shown in Figure 4 to explain the fine-grained estimator formulated in (3.4). Consider the Reset Cliff MDP with state space $\mathcal{S} = \{\textcircled{1}, \textcircled{2}, \textcircled{b}\}$ where \textcircled{b} is the bad state, and action space $\mathcal{A} = \{g, b\}$ where g and b denote the green and blue action, respectively. For simplicity, the planning horizon is $H = 2$. The number of expert demonstrations $m = 100$ and the initial state distribution $\rho = (\rho(\textcircled{1}), \rho(\textcircled{2}), \rho(\textcircled{b})) = (\frac{1}{100}, \frac{99}{100}, 0)$. Consider the dataset \mathcal{D} includes 97 trajectories of $\text{tr}^1 = (\textcircled{2}, g, \textcircled{2}, g)$, 2 trajectories of $\text{tr}^2 = (\textcircled{1}, g, \textcircled{2}, g)$ and 1 trajectory of $\text{tr}^3 = (\textcircled{2}, g, \textcircled{1}, g)$.

First of all, let us consider the maximum likelihood estimator.

$$\begin{aligned} \text{at time step } h = 1: \quad & \left(\widehat{P}_1^{\pi^E} \circ \mathcal{D} \right) (\textcircled{1}, g) = \frac{1}{50}, \quad \left(\widehat{P}_1^{\pi^E} \circ \mathcal{D} \right) (\textcircled{2}, g) = \frac{49}{50}, \\ \text{at time step } h = 2: \quad & \left(\widehat{P}_2^{\pi^E} \circ \mathcal{D} \right) (\textcircled{1}, g) = \frac{1}{100}, \quad \left(\widehat{P}_2^{\pi^E} \circ \mathcal{D} \right) (\textcircled{2}, g) = \frac{99}{100}. \end{aligned}$$

Hence, ℓ_1 -norm estimation error $\sum_{h=1}^2 \left\| P_h^{\pi^E} - \widehat{P}_h^{\pi^E} \right\|_1 = 0.02$.

Now we consider the fine-grained estimator shown in (3.4). In particular, we split \mathcal{D} into two equals parts $\mathcal{D} = \mathcal{D}_1 \cup \mathcal{D}_1^c$: \mathcal{D}_1 contains 49 trajectories of $\text{tr}^1 = (\textcircled{2}, g, \textcircled{2}, g)$ and 1 trajectory of $\text{tr}^2 = (\textcircled{1}, g, \textcircled{2}, g)$; \mathcal{D}_1^c contains 48 trajectories of $\text{tr}^1 = (\textcircled{2}, g, \textcircled{2}, g)$, 1 trajectory of $\text{tr}^2 = (\textcircled{1}, g, \textcircled{2}, g)$ and 1 trajectory of $\text{tr}^3 = (\textcircled{2}, g, \textcircled{1}, g)$. Hence, we can enumerate the trajectories to obtain that $\text{Tr}_{\mathcal{D}_1} = \{(\textcircled{1}, g) (\textcircled{2}, g)\}$, $\text{Tr}_{\mathcal{D}_1^c} = \{(\textcircled{1}, g, \textcircled{2}, g) (\textcircled{2}, g, \textcircled{2}, g)\}$.

$$\begin{aligned} \text{at time step } h = 1: \quad & \left(\widetilde{P}_1^{\pi^E} \circ \mathcal{D} \right) (\textcircled{1}, g) = \mathbb{P}^{\pi^E} ((\textcircled{1}, g)) = \frac{1}{100}, \\ \text{at time step } h = 1: \quad & \left(\widetilde{P}_1^{\pi^E} \circ \mathcal{D} \right) (\textcircled{2}, g) = \mathbb{P}^{\pi^E} ((\textcircled{2}, g)) = \frac{99}{100}, \\ \text{at time step } h = 2: \quad & \left(\widetilde{P}_2^{\pi^E} \circ \mathcal{D} \right) (\textcircled{1}, g) = \left(\widehat{P}_2^{\pi^E} \circ \mathcal{D}_1^c \right) (\textcircled{1}, g) = \frac{1}{50}, \\ \text{at time step } h = 2: \quad & \left(\widetilde{P}_2^{\pi^E} \circ \mathcal{D} \right) (\textcircled{2}, g) = \mathbb{P}^{\pi^E} ((\textcircled{1}, g, \textcircled{2}, g)) + \mathbb{P}^{\pi^E} ((\textcircled{2}, g, \textcircled{2}, g)) = \frac{99}{100}. \end{aligned}$$

Therefore, we see ℓ_1 -norm estimation error $\sum_{h=1}^2 \left\| P_h^{\pi^E} - \widetilde{P}_h^{\pi^E} \right\|_1 = 0.01$.

D Proof of Results in Section 3

D.1 Proof of Lemma 3.2

Proof. Our target is to upper bound the estimation error of $\tilde{P}_h^{\pi^E}$:

$$\sum_{h=1}^H \left\| \tilde{P}_h^{\pi^E}(s, a) - P_h^{\pi^E}(s, a) \right\|_1 = \sum_{h=1}^H \sum_{(s, a) \in \mathcal{S} \times \mathcal{A}} \left| \tilde{P}_h^{\pi^E}(s, a) - P_h^{\pi^E}(s, a) \right|,$$

where $\tilde{P}_h^{\pi^E}$ is defined in (3.4):

$$(\tilde{P}_h^{\pi^E} \circ \mathcal{D})(s, a) := \sum_{\mathbf{tr}_h \in \text{Tr}_h^{\mathcal{D}_1}} \mathbb{P}^{\pi^E}(\mathbf{tr}_h) \mathbb{I}\{\mathbf{tr}_h(s_h, a_h) = (s, a)\} + (\hat{P}_h^{\pi^E} \circ \mathcal{D}_1^c)(s, a)$$

where $\text{Tr}_h^{\mathcal{D}_1}$ is the set of trajectories that totally agrees with certain trajectories in \mathcal{D}_1 up to time step h (i.e., $\text{Tr}_h^{\mathcal{D}_1} = \{\mathbf{tr}_h : \mathbf{tr}_h \in \mathcal{D}_1\}$). Similarly, for $P_h^{\pi^E}$, we have the following decomposition:

$$P_h^{\pi^E}(s, a) = \sum_{\mathbf{tr}_h \in \text{Tr}_h^{\mathcal{D}_1}} \mathbb{P}^{\pi^E}(\mathbf{tr}_h) \mathbb{I}\{\mathbf{tr}_h(s_h, a_h) = (s, a)\} + \sum_{\mathbf{tr}_h \notin \text{Tr}_h^{\mathcal{D}_1}} \mathbb{P}^{\pi^E}(\mathbf{tr}_h) \mathbb{I}\{\mathbf{tr}_h(s_h, a_h) = (s, a)\}.$$

Consequently, we obtain for any $(s, a) \in \mathcal{S} \times \mathcal{A}, h \in [H]$,

$$\begin{aligned} & \left| \tilde{P}_h^{\pi^E}(s, a) - P_h^{\pi^E}(s, a) \right| \\ &= \left| \tilde{P}_h^{\pi^E}(s, a) - \sum_{\mathbf{tr}_h \in \text{Tr}_h^{\mathcal{D}_1}} \mathbb{P}^{\pi^E}(\mathbf{tr}_h) \mathbb{I}\{\mathbf{tr}_h(s_h, a_h) = (s, a)\} - \sum_{\mathbf{tr}_h \notin \text{Tr}_h^{\mathcal{D}_1}} \mathbb{P}^{\pi^E}(\mathbf{tr}_h) \mathbb{I}\{\mathbf{tr}_h(s_h, a_h) = (s, a)\} \right| \\ &= \left| (\hat{P}_h^{\pi^E} \circ \mathcal{D}_1^c)(s, a) - \sum_{\mathbf{tr}_h \notin \text{Tr}_h^{\mathcal{D}_1}} \mathbb{P}^{\pi^E}(\mathbf{tr}_h) \mathbb{I}\{\mathbf{tr}_h(s_h, a_h) = (s, a)\} \right|. \end{aligned}$$

That is, the estimation error is caused by the unknown expert actions in trajectories that does not fully match with any trajectory in \mathcal{D}_1 . Since π^E is a deterministic policy, which implies we can write $(s, a) = (s, \pi^E(s))$, we obtain that

$$\begin{aligned} & \left| (\hat{P}_h^{\pi^E} \circ \mathcal{D}_1^c)(s, a) - \sum_{\mathbf{tr}_h \notin \text{Tr}_h^{\mathcal{D}_1}} \mathbb{P}^{\pi^E}(\mathbf{tr}_h) \mathbb{I}\{\mathbf{tr}_h(s_h, a_h) = (s, a)\} \right| \\ &= \left| (\hat{P}_h^{\pi^E} \circ \mathcal{D}_1^c)(s, \pi^E(s)) - \sum_{\mathbf{tr}_h \notin \text{Tr}_h^{\mathcal{D}_1}} \mathbb{P}^{\pi^E}(\mathbf{tr}_h) \mathbb{I}\{\mathbf{tr}_h(s_h, a_h) = (s, \pi^E(s))\} \right|. \end{aligned} \tag{D.1}$$

Fix \mathcal{D}_1 , we see that the above error bound corresponds to the Bernoulli random variables estimation. In particular, for a sample truncated trajectory \mathbf{tr}_h , let E_h^s be the event that \mathbf{tr}_h agrees with expert policy at state s at time step h but is not in $\text{Tr}_h^{\mathcal{D}_1}$, that is,

$$E_h^s = \mathbb{I}\{\mathbf{tr}_h(s_h, a_h) = (s, \pi_h^E(s)) \cap \mathbf{tr}_h \notin \text{Tr}_h^{\mathcal{D}_1}\}.$$

We will consider E_h^s is measured by the stochastic process induced by π^E ; correspondingly, its probability is denoted as $\mathbb{P}^{\pi^E}(E_h^s)$. We will show that $\mathbb{P}^{\pi^E}(E_h^s)$ is well controlled so that applying Chernoff's bound [Vershynin, 2018] can yield a better sample complexity than Hoeffding's inequality used for direct maximum likelihood estimation.

Lemma D.1 (Chernoff's bound [Vershynin, 2018]). *Let $\bar{X} = \frac{1}{n} \sum_{i=1}^n X_i$, where X_i is a Bernoulli random variable with $\mathbb{P}(X_i = 1) = p_i$ and $\mathbb{P}(X_i = 0) = 1 - p_i$ for $i \in [n]$. Furthermore, assume these random variables are independent. Let $\mu = \mathbb{E}[\bar{X}] = \frac{1}{n} \sum_{i=1}^n p_i$. Then for $0 < t \leq 1$,*

$$\mathbb{P}(|\bar{X} - \mu| \geq t\mu) \leq 2 \exp\left(-\frac{\mu nt^2}{3}\right).$$

Applying Lemma D.1 to (D.1) and taking an union bound, we have with probability at least $1 - \delta/(2|\mathcal{S}|H)$ with $\delta \in (0, 1)$ over the randomness of the dataset \mathcal{D}_1^c , for each $h \in [H], s \in \mathcal{S}$, the following inequality holds,

$$\begin{aligned} & \left| \left(\widehat{P}_h^{\pi^E} \circ \mathcal{D}_1^c \right) (s, \pi^E(s)) - \sum_{\mathbf{tr}_h \notin \text{Tr}_h^{\mathcal{D}_1}} \mathbb{P}^{\pi^E}(\mathbf{tr}_h) \mathbb{I}\{\mathbf{tr}_h(s_h, a_h) = (s, \pi^E(s))\} \right| \\ & \leq \sqrt{\mathbb{P}^{\pi^E}(E_h^s) \frac{3 \log(4|\mathcal{S}|H/\delta)}{m}}. \end{aligned}$$

Therefore, we obtain with probability at least $1 - \delta/2$ over the randomness of the dataset \mathcal{D}_1^c , we have

$$\begin{aligned} \sum_{h=1}^H \sum_{(s,a) \in \mathcal{S} \times \mathcal{A}} \left| \widetilde{P}_h^{\pi^E}(s, a) - P_h^{\pi^E}(s, a) \right| & \leq \sum_{h=1}^H \sum_{s \in \mathcal{S}} \sqrt{\mathbb{P}^{\pi^E}(E_h^s) \frac{3 \log(4|\mathcal{S}|H/\delta)}{m}} \\ & \leq \sum_{h=1}^H \sqrt{\sum_{s \in \mathcal{S}} \mathbb{P}^{\pi^E}(E_h^s) \frac{3|\mathcal{S}| \log(4|\mathcal{S}|H/\delta)}{m}}, \end{aligned}$$

where the last step follows the Cauchy–Schwarz inequality. It remains to upper bound $\sum_{s \in \mathcal{S}} \mathbb{P}^{\pi^E}(E_h^s)$ for all $h \in [H]$. To this end, we define the event $G_h^{\mathcal{D}_1}$ that policy π^E visits states uncovered in \mathcal{D}_1 up to time step h . Formally, $G_h^{\mathcal{D}_1} = \mathbb{I}\{\exists h' \leq h, s_{h'} \notin \mathcal{S}_{h'}(\mathcal{D}_1)\}$, where $\mathcal{S}_h(\mathcal{D}_1)$ is the set of states in \mathcal{D}_1 at time step h . Then, for all $h \in [H]$, we have

$$\sum_{s \in \mathcal{S}} \mathbb{P}^{\pi^E}(E_h^s) = \mathbb{P}^{\pi^E}(G_h^{\mathcal{D}_1}) \leq \mathbb{P}(G_H^{\mathcal{D}_1}).$$

The last inequality holds since $G_h^{\mathcal{D}_1} \subseteq G_H^{\mathcal{D}_1}$ for all $h \in [H]$. Conditioned on \mathcal{D}_1 , we further have

$$\mathbb{P}(G_H^{\mathcal{D}_1}) \leq \sum_{h=1}^H \sum_{s \in \mathcal{S}} P_h^{\pi}(s) \mathbb{I}\{s \notin \mathcal{S}_h(\mathcal{D}_1)\}.$$

We note that RHS is so-called *missing mass* [McAllester and Ortiz, 2003, Rajaraman et al., 2020]. In summary, we arrive at, with probability $1 - \delta/2$ over the randomness of the dataset \mathcal{D}_1^c ,

$$\sum_{h=1}^H \sum_{(s,a) \in \mathcal{S} \times \mathcal{A}} \left| \widetilde{P}_h^{\pi^E}(s, a) - P_h^{\pi^E}(s, a) \right| \leq \sum_{h=1}^H \sqrt{\sum_{h=1}^H \sum_{s \in \mathcal{S}} P_h^{\pi}(s) \mathbb{I}\{s \notin \mathcal{S}_h(\mathcal{D}_1)\} \frac{3|\mathcal{S}| \log(4|\mathcal{S}|H/\delta)}{m}}.$$

We first consider the expectation $\mathbb{E}[\sum_{h=1}^H \sum_{s \in \mathcal{S}} P_h^{\pi}(s) \mathbb{I}\{s \notin \mathcal{S}_h(\mathcal{D}_1)\}]$, where the expectation is taken over the expert dataset \mathcal{D}_1 .

$$\mathbb{E} \left[\sum_{h=1}^H \sum_{s \in \mathcal{S}} P_h^{\pi}(s) \mathbb{I}\{s \notin \mathcal{S}_h(\mathcal{D}_1)\} \right] \leq \sum_{h=1}^H \sum_{s \in \mathcal{S}} P_h^{\pi^E}(s) \left(1 - P_h^{\pi^E}(s)\right)^{m/2} \leq \frac{8|\mathcal{S}|H}{9m},$$

where the last step uses the numerical inequality⁶ $\max_{x \in [0,1]} x(1-x)^m \leq \frac{1}{1+m} \left(1 - \frac{1}{m}\right)^m \leq \frac{4}{9m}$. To transform the bound in expectation to a high probability form, we use the following concentration bound from [Rajaraman et al., 2020], which is based on [McAllester and Ortiz, 2003].

Lemma D.2 (Concentration inequality for missing mass[Rajaraman et al., 2020]). *Suppose that*

$$\mathbb{E} \left[\sum_{h=1}^H \sum_{s \in \mathcal{S}} P_h^{\pi}(s) \mathbb{I}\{s \notin \mathcal{S}_h(\mathcal{D}_1)\} \right] \leq \frac{8|\mathcal{S}|H}{9m}.$$

Fix $\delta \in (0, 1)$ with $\delta \in (0, \min\{1, H/10\})$, with probability at least $1 - \delta$ over the randomness of the expert dataset \mathcal{D}_1 , we have

$$\sum_{h=1}^H \sum_{s \in \mathcal{S}} P_h^{\pi}(s) \mathbb{I}\{s \notin \mathcal{S}_h(\mathcal{D}_1)\} \leq \frac{8|\mathcal{S}|H}{9m} + \frac{6\sqrt{|\mathcal{S}|H \log(H/\delta)}}{m}.$$

⁶The first inequality is based on basic calculus and the second inequality is based on the fact that $(1 - 1/x)^x \leq 1/e \leq 4/9$ while $x \geq 1$.

With Lemma D.2, with probability at least $1 - \delta$ with $\delta \in (0, \min\{1, H/5\})$, we have

$$\begin{aligned} & \sum_{h=1}^H \sum_{(s,a) \in \mathcal{S} \times \mathcal{A}} \left| \tilde{P}_h^{\pi^E}(s, a) - P_h^{\pi^E}(s, a) \right| \\ & \leq \sum_{h=1}^H \sqrt{\left(\frac{8|\mathcal{S}|H}{9m} + \frac{6\sqrt{|\mathcal{S}|H} \log(2H/\delta)}{m} \right) \frac{3|\mathcal{S}| \log(4|\mathcal{S}|H/\delta)}{m}} \\ & \leq \frac{H^{3/2}|\mathcal{S}|}{m} \log^{1/2} \left(\frac{4|\mathcal{S}|H}{\delta} \right) \sqrt{\frac{8}{3} + 18 \log(2H/\delta)}. \end{aligned}$$

Rearranging yields the desired result. \square

D.2 Proof of Theorem 3.1

Before we prove Theorem 3.1, we first state two key lemmas: Lemma D.3 and Lemma D.4.

Lemma D.3. *Consider the adversarial imitation learning approach displayed in Algorithm 1, then we have*

$$\sum_{t=1}^T f^{(t)}(w^{(t)}) - \min_{w \in \mathcal{W}} \sum_{t=1}^T f^{(t)}(w) \leq 2H \sqrt{2|\mathcal{S}||\mathcal{A}|T},$$

where $f^{(t)}(w) = \sum_{h=1}^H \sum_{(s,a) \in \mathcal{S} \times \mathcal{A}} w_h(s, a) \left(P_h^{\pi^{(t)}}(s, a) - \tilde{P}_h^{\pi^E}(s, a) \right)$.

Proof. Lemma D.3 is a direct consequence of the regret bound of online gradient descend [Shalev-Shwartz, 2012]. For each $w \in \mathcal{W}$, it is easy to verify that the ℓ_2 -norm of w has an upper bound, i.e., $\|w\|_2 \leq \sqrt{H|\mathcal{S}||\mathcal{A}|}$. Recall the definition of $f^{(t)}(w)$:

$$f^{(t)}(w) = \sum_{h=1}^H \sum_{(s,a) \in \mathcal{S} \times \mathcal{A}} w_h(s, a) \left(P_h^{\pi^{(t)}}(s, a) - \tilde{P}_h^{\pi^E}(s, a) \right).$$

We upper bound the ℓ_2 -norm of the gradient of $f^{(t)}(w)$.

Let \tilde{P}_h^1 and \tilde{P}_h^2 be the first and the second part in $\tilde{P}_h^{\pi^E}$ defined in (3.4). Then,

$$\begin{aligned} \left\| \nabla_w f^{(t)}(w) \right\|_2 &= \sqrt{\sum_{h=1}^H \sum_{s,a} \left(P_h^{\pi^{(t)}}(s, a) - \tilde{P}_h^{\pi^E}(s, a) \right)^2} \\ &= \sqrt{\sum_{h=1}^H \sum_{s,a} \left(P_h^{\pi^{(t)}}(s, a) - \tilde{P}_h^1(s, a) - \tilde{P}_h^2(s, a) \right)^2} \\ &\leq \sqrt{\sum_{h=1}^H 3 \sum_{s,a} \left(P_h^{\pi^{(t)}}(s, a) \right)^2 + \left(\tilde{P}_h^1(s, a) \right)^2 + \left(\tilde{P}_h^2(s, a) \right)^2} \\ &\leq \sqrt{\sum_{h=1}^H 3 \left(\left\| P_h^{\pi^{(t)}} \right\|_1 + \left\| \tilde{P}_h^1 \right\|_1 + \left\| \tilde{P}_h^2 \right\|_1 \right)} \\ &\leq 2\sqrt{H}, \end{aligned}$$

where the first inequality follows $(a + b + c)^2 \leq 3(a^2 + b^2 + c^2)$ and the second inequality is based on that $x^2 \leq |x|$ if $0 \leq x \leq 1$.

Invoking Corollary 2.7 in [Shalev-Shwartz, 2012] with $B = \sqrt{H|\mathcal{S}||\mathcal{A}|}$ and $L = 2\sqrt{H}$ finishes the proof. \square

Lemma D.4. *Consider the transition-aware adversarial imitation learning approach displayed in Algorithm 1 and $\bar{\pi}$ is the output policy, then we have*

$$\sum_{h=1}^H \left\| P_h^{\bar{\pi}}(s, a) - \tilde{P}_h^{\pi^E}(s, a) \right\|_1 \leq \min_{\pi \in \Pi} \sum_{h=1}^H \left\| P_h^{\pi}(s, a) - \tilde{P}_h^{\pi^E}(s, a) \right\|_1 + 2H \sqrt{\frac{2|\mathcal{S}||\mathcal{A}|}{T}} + \varepsilon_{\text{opt}}.$$

Proof of Lemma D.4. With the dual representation of ℓ_1 -norm, we have

$$\min_{\pi \in \Pi} \sum_{h=1}^H \left\| P_h^\pi(s, a) - \tilde{P}_h^{\pi^E}(s, a) \right\|_1 = \min_{\pi \in \Pi} \max_{w \in \mathcal{W}} \sum_{h=1}^H \sum_{(s, a) \in \mathcal{S} \times \mathcal{A}} w_h(s, a) \left(\tilde{P}_h^{\pi^E}(s, a) - P_h^\pi(s, a) \right).$$

Since the above objective is linear w.r.t both w and P_h^π , invoking the minimax theorem [Bertsekas, 2016] yields

$$\begin{aligned} & \min_{\pi \in \Pi} \max_{w \in \mathcal{W}} \sum_{h=1}^H \sum_{(s, a) \in \mathcal{S} \times \mathcal{A}} w_h(s, a) \left(\tilde{P}_h^{\pi^E}(s, a) - P_h^\pi(s, a) \right) \\ &= \max_{w \in \mathcal{W}} \min_{\pi \in \Pi} \sum_{h=1}^H \sum_{(s, a) \in \mathcal{S} \times \mathcal{A}} w_h(s, a) \left(\tilde{P}_h^{\pi^E}(s, a) - P_h^\pi(s, a) \right) \\ &= - \min_{w \in \mathcal{W}} \max_{\pi \in \Pi} \sum_{h=1}^H \sum_{(s, a) \in \mathcal{S} \times \mathcal{A}} w_h(s, a) \left(P_h^\pi(s, a) - \tilde{P}_h^{\pi^E}(s, a) \right), \end{aligned}$$

where the last step follows the property that for a function f , $-\max_x f(x) = \min_x -f(x)$. Therefore, we have

$$\min_{\pi \in \Pi} \sum_{h=1}^H \left\| P_h^\pi(s, a) - \tilde{P}_h^{\pi^E}(s, a) \right\|_1 = - \min_{w \in \mathcal{W}} \max_{\pi \in \Pi} \sum_{h=1}^H \sum_{(s, a) \in \mathcal{S} \times \mathcal{A}} w_h(s, a) \left(P_h^\pi(s, a) - \tilde{P}_h^{\pi^E}(s, a) \right). \quad (\text{D.2})$$

Then we consider the term $\min_{w \in \mathcal{W}} \max_{\pi \in \Pi} \sum_{h=1}^H \sum_{(s, a) \in \mathcal{S} \times \mathcal{A}} w_h(s, a) \left(P_h^\pi(s, a) - \tilde{P}_h^{\pi^E}(s, a) \right)$.

$$\begin{aligned} & \min_{w \in \mathcal{W}} \max_{\pi \in \Pi} \sum_{h=1}^H \sum_{(s, a) \in \mathcal{S} \times \mathcal{A}} w_h(s, a) \left(P_h^\pi(s, a) - \tilde{P}_h^{\pi^E}(s, a) \right) \\ & \leq \max_{\pi \in \Pi} \sum_{h=1}^H \sum_{(s, a) \in \mathcal{S} \times \mathcal{A}} \left(\frac{1}{T} \sum_{t=1}^T w_h^{(t)}(s, a) \right) \left(P_h^\pi(s, a) - \tilde{P}_h^{\pi^E}(s, a) \right) \\ & \leq \frac{1}{T} \sum_{t=1}^T \max_{\pi \in \Pi} \sum_{h=1}^H \sum_{(s, a) \in \mathcal{S} \times \mathcal{A}} w_h^{(t)}(s, a) \left(P_h^\pi(s, a) - \tilde{P}_h^{\pi^E}(s, a) \right). \end{aligned}$$

At iteration t , $\pi^{(t)}$ is the approximately optimal policy regarding reward function $w^{(t)}$ with an optimization error of ε_{opt} . Then we obtain that

$$\begin{aligned} & \frac{1}{T} \sum_{t=1}^T \max_{\pi \in \Pi} \sum_{h=1}^H \sum_{(s, a) \in \mathcal{S} \times \mathcal{A}} w_h^{(t)}(s, a) \left(P_h^\pi(s, a) - \tilde{P}_h^{\pi^E}(s, a) \right) \\ & \leq \frac{1}{T} \sum_{t=1}^T \sum_{h=1}^H \sum_{(s, a) \in \mathcal{S} \times \mathcal{A}} w_h^{(t)}(s, a) \left(P_h^{\pi^{(t)}}(s, a) - \tilde{P}_h^{\pi^E}(s, a) \right) + \varepsilon_{\text{opt}}. \end{aligned}$$

Applying Lemma D.3 yields that

$$\begin{aligned} & \frac{1}{T} \sum_{t=1}^T \sum_{h=1}^H \sum_{(s, a) \in \mathcal{S} \times \mathcal{A}} w_h^{(t)}(s, a) \left(P_h^{\pi^{(t)}}(s, a) - \tilde{P}_h^{\pi^E}(s, a) \right) \\ & \leq \min_{w \in \mathcal{W}} \frac{1}{T} \sum_{t=1}^T \sum_{h=1}^H \sum_{(s, a) \in \mathcal{S} \times \mathcal{A}} w_h(s, a) \left(P_h^{\pi^{(t)}}(s, a) - \tilde{P}_h^{\pi^E}(s, a) \right) + 2H\sqrt{\frac{2|\mathcal{S}||\mathcal{A}|}{T}} \\ & = \min_{w \in \mathcal{W}} \sum_{h=1}^H \sum_{(s, a) \in \mathcal{S} \times \mathcal{A}} w_h(s, a) \left(\frac{1}{T} \sum_{t=1}^T P_h^{\pi^{(t)}}(s, a) - \tilde{P}_h^{\pi^E}(s, a) \right) + 2H\sqrt{\frac{2|\mathcal{S}||\mathcal{A}|}{T}} \\ & = \min_{w \in \mathcal{W}} \sum_{h=1}^H \sum_{(s, a) \in \mathcal{S} \times \mathcal{A}} w_h(s, a) \left(P_h^{\bar{\pi}}(s, a) - \tilde{P}_h^{\pi^E}(s, a) \right) + 2H\sqrt{\frac{2|\mathcal{S}||\mathcal{A}|}{T}}. \end{aligned}$$

Note that $\bar{\pi}$ is induced by the mean state-action distribution, i.e., $\bar{\pi}_h(a|s) = \bar{P}_h(s, a) / \sum_a \bar{P}_h(s, a)$, where $\bar{P}_h(s, a) = \frac{1}{T} \sum_{t=1}^T P_h^{\pi^{(t)}}(s, a)$. Based on Proposition 3.1 in [Ho and Ermon, 2016], we have that $P_h^{\bar{\pi}}(s, a) = \bar{P}_h(s, a)$, and hence the last equation holds. Combined with (D.2), we have that

$$\begin{aligned} & \min_{\pi \in \Pi} \sum_{h=1}^H \left\| P_h^{\pi}(s, a) - \tilde{P}_h^{\pi^E}(s, a) \right\|_1 \\ & \geq - \min_{w \in \mathcal{W}} \sum_{h=1}^H \sum_{(s, a) \in \mathcal{S} \times \mathcal{A}} w_h(s, a) \left(P_h^{\bar{\pi}}(s, a) - \tilde{P}_h^{\pi^E}(s, a) \right) - 2H\sqrt{\frac{2|\mathcal{S}||\mathcal{A}|}{T}} - \varepsilon_{\text{opt}} \\ & = \max_{w \in \mathcal{W}} \sum_{h=1}^H \sum_{(s, a) \in \mathcal{S} \times \mathcal{A}} w_h(s, a) \left(\tilde{P}_h^{\pi^E}(s, a) - P_h^{\bar{\pi}}(s, a) \right) - 2H\sqrt{\frac{2|\mathcal{S}||\mathcal{A}|}{T}} - \varepsilon_{\text{opt}} \\ & = \left\| \tilde{P}_h^{\pi^E}(s, a) - P_h^{\bar{\pi}}(s, a) \right\|_1 - 2H\sqrt{\frac{2|\mathcal{S}||\mathcal{A}|}{T}} - \varepsilon_{\text{opt}}, \end{aligned}$$

where the last step again utilizes the dual representation of ℓ_1 -norm. We complete the proof. \square

Proof of Theorem 3.1. Let $\bar{\pi}$ be the policy output by Algorithm 1. With Lemma D.4, we establish the upper bound on the ℓ_1 deviation between $P_h^{\bar{\pi}}(s, a)$ and $\tilde{P}_h^{\pi^E}(s, a)$.

$$\sum_{h=1}^H \left\| P_h^{\bar{\pi}}(s, a) - \tilde{P}_h^{\pi^E}(s, a) \right\|_1 \leq \min_{\pi \in \Pi} \sum_{h=1}^H \left\| P_h^{\pi}(s, a) - \tilde{P}_h^{\pi^E}(s, a) \right\|_1 + 2H\sqrt{\frac{2|\mathcal{S}||\mathcal{A}|}{T}} + \varepsilon_{\text{opt}}.$$

Since $\pi^E \in \Pi$, we further obtain that

$$\sum_{h=1}^H \left\| P_h^{\bar{\pi}}(s, a) - \tilde{P}_h^{\pi^E}(s, a) \right\|_1 \leq \sum_{h=1}^H \left\| P_h^{\pi^E}(s, a) - \tilde{P}_h^{\pi^E}(s, a) \right\|_1 + 2H\sqrt{\frac{2|\mathcal{S}||\mathcal{A}|}{T}} + \varepsilon_{\text{opt}}.$$

Fix $\varepsilon \in (0, H)$ and $\delta \in (0, 1)$, when the number of trajectories in \mathcal{D} satisfies that $m \gtrsim \frac{|\mathcal{S}|H^{3/2}}{\varepsilon} \log\left(\frac{|\mathcal{S}|H}{\delta}\right)$, with probability at least $1 - \delta$, we have

$$\sum_{h=1}^H \left\| P_h^{\pi^E}(s, a) - \tilde{P}_h^{\pi^E}(s, a) \right\|_1 \leq \frac{\varepsilon}{4}.$$

Moreover, with $T \gtrsim \frac{|\mathcal{S}||\mathcal{A}|H^2}{\varepsilon^2}$ and $\varepsilon_{\text{opt}} \leq \frac{\varepsilon}{2}$, we can obtain that

$$\sum_{h=1}^H \left\| P_h^{\bar{\pi}}(s, a) - \tilde{P}_h^{\pi^E}(s, a) \right\|_1 \leq \frac{\varepsilon}{4} + \frac{\varepsilon}{4} + \varepsilon_{\text{opt}} \leq \varepsilon.$$

Finally, applying Lemma 3.1 upper bounds the policy value gap by the state-action distribution error. \square

E Proof of Results in Section 4

E.1 Proof of Lemma 4.1

Proof. Let $\Pi(\mathcal{D}_1)$ denote the set of policies, each of which exactly takes expert action on states contained in \mathcal{D}_1 . Fix $\pi \in \Pi(\mathcal{D}_1)$, $h \in [H]$ and $(s, a) \in \mathcal{S} \times \mathcal{A}$, we consider the probability $\mathbb{P}^{\pi^E}(\mathbf{tr}_h)$ of a truncated trajectory $\mathbf{tr}_h \in \text{Tr}_h^{\mathcal{D}_1}$. Since π exactly takes expert action on states contained in \mathcal{D}_1 , we have

$$\begin{aligned} & \mathbb{P}^{\pi^E}(\mathbf{tr}_h) \\ &= \rho(\mathbf{tr}_h(s_1))\pi_1^E(\mathbf{tr}_h(a_1)|\mathbf{tr}(s_1)) \prod_{\ell=1}^{h-1} P_\ell(\mathbf{tr}_h(s_{\ell+1})|\mathbf{tr}_h(s_\ell), \mathbf{tr}_h(a_\ell))\pi_{\ell+1}^E(\mathbf{tr}_h(a_{\ell+1})|\mathbf{tr}_h(s_{\ell+1})) \\ &= \rho(\mathbf{tr}_h(s_1))\pi_1(\mathbf{tr}_h(a_1)|\mathbf{tr}(s_1)) \prod_{\ell=1}^{h-1} P_\ell(\mathbf{tr}_h(s_{\ell+1})|\mathbf{tr}_h(s_\ell), \mathbf{tr}_h(a_\ell))\pi_{\ell+1}(\mathbf{tr}_h(a_{\ell+1})|\mathbf{tr}_h(s_{\ell+1})) \\ &= \mathbb{P}^\pi(\mathbf{tr}_h). \end{aligned}$$

Therefore, we obtain that

$$\sum_{\mathbf{tr}_h \in \text{Tr}_h^{\mathcal{D}_1}} \mathbb{P}^{\pi^E}(\mathbf{tr}_h) \mathbb{I}\{\mathbf{tr}_h(s_h, a_h) = (s, a)\} = \sum_{\mathbf{tr}_h \in \text{Tr}_h^{\mathcal{D}_1}} \mathbb{P}^\pi(\mathbf{tr}_h) \mathbb{I}\{\mathbf{tr}_h(s_h, a_h) = (s, a)\},$$

which completes the proof. \square

E.2 Proof of Theorem 4.1

To prove Theorem 4.1, we first introduce the following useful lemmas.

We first present our theoretical result on the expert sample complexity and interaction complexity required by the new estimator shown in (4.1) under the unknown transition setting.

Lemma E.1. *Given expert dataset \mathcal{D} and \mathcal{D} is divided into two equal subsets, i.e., $\mathcal{D} = \mathcal{D}_1 \cup \mathcal{D}_1^c$ with $|\mathcal{D}_1| = |\mathcal{D}_1^c| = m/2$. Fix $\pi \in \Pi(\mathcal{D}_1)$, let \mathcal{D}' be the dataset collected by π and $|\mathcal{D}'| = n$. Fix $\varepsilon \in (0, 1)$ and $\delta \in (0, 1)$; suppose $H \geq 5$. Consider the estimator $\tilde{P}_h^{\pi^E}$ shown in (4.1), if the expert sample complexity (i.e., $|\mathcal{D}|$) and the interaction complexity (i.e., $|\mathcal{D}'|$) satisfies*

$$m \gtrsim \frac{H^{3/2}|\mathcal{S}|}{\varepsilon} \log\left(\frac{|\mathcal{S}|H}{\delta}\right), \quad n \gtrsim \frac{H^2|\mathcal{S}|}{\varepsilon^2} \log\left(\frac{|\mathcal{S}|H}{\delta}\right),$$

then with probability at least $1 - \delta$, we have

$$\sum_{h=1}^H \left\| \tilde{P}_h^{\pi^E}(s, a) - P_h^{\pi^E}(s, a) \right\|_1 \leq \varepsilon.$$

Proof. We aim to upper bound the estimation error.

$$\sum_{h=1}^H \left\| \tilde{P}_h^{\pi^E}(s, a) - P_h^{\pi^E}(s, a) \right\|_1.$$

Recall the definition of the estimator $\tilde{P}_h^{\pi^E}(s, a)$.

$$(\tilde{P}_h^{\pi^E} \circ \mathcal{D})(s, a) := (\hat{P}_h^{\pi^E} \circ \mathcal{D}') (s, a) + (\hat{P}_h^{\pi^E} \circ \mathcal{D}_1^c)(s, a),$$

where

$$(\hat{P}_h^{\pi^E} \circ \mathcal{D}') (s, a) = \frac{\sum_{\mathbf{tr}_h \in \mathcal{D}'} \mathbb{I}\{\mathbf{tr}_h(s_h, a_h) = (s, a), \mathbf{tr}_h \in \text{Tr}_h^{\mathcal{D}_1}\}}{|\mathcal{D}'|}$$

and

$$(\hat{P}_h^{\pi^E} \circ \mathcal{D}_1^c)(s, a) = \frac{\sum_{\mathbf{tr}_h \in \mathcal{D}_1^c} \mathbb{I}\{\mathbf{tr}_h(s_h, a_h) = (s, a), \mathbf{tr}_h \notin \text{Tr}_h^{\mathcal{D}_1}\}}{|\mathcal{D}_1^c|}.$$

Similarly, we utilize the decomposition of $P_h^{\pi^E}(s, a)$ as we have done in the proof of Lemma 3.2.

$$P_h^{\pi^E}(s, a) = \sum_{\mathbf{tr}_h \in \text{Tr}_h^{\mathcal{D}_1}} \mathbb{P}^{\pi^E}(\mathbf{tr}_h) \mathbb{I}\{\mathbf{tr}_h(s_h, a_h) = (s, a)\} + \sum_{\mathbf{tr}_h \notin \text{Tr}_h^{\mathcal{D}_1}} \mathbb{P}^{\pi^E}(\mathbf{tr}_h) \mathbb{I}\{\mathbf{tr}_h(s_h, a_h) = (s, a)\}.$$

Then, for any $h \in [H]$ and $(s, a) \in \mathcal{S} \times \mathcal{A}$, we have

$$\left| \tilde{P}_h^{\pi^E}(s, a) - P_h^{\pi^E}(s, a) \right| \leq \left| \left(\hat{P}_h^{\pi^E} \circ \mathcal{D}' \right) (s, a) - \sum_{\mathbf{tr}_h \in \text{Tr}_h^{\mathcal{D}_1}} \mathbb{P}^{\pi^E}(\mathbf{tr}_h) \mathbb{I}\{\mathbf{tr}_h(s_h, a_h) = (s, a)\} \right| \\ + \left| \left(\hat{P}_h^{\pi^E} \circ \mathcal{D}_1^c \right) (s, a) - \sum_{\mathbf{tr}_h \notin \text{Tr}_h^{\mathcal{D}_1}} \mathbb{P}^{\pi^E}(\mathbf{tr}_h) \mathbb{I}\{\mathbf{tr}_h(s_h, a_h) = (s, a)\} \right|.$$

Thus, we can upper bound the estimation error.

$$\sum_{h=1}^H \left\| \tilde{P}_h^{\pi^E}(s, a) - P_h^{\pi^E}(s, a) \right\|_1 \\ \leq \underbrace{\sum_{h=1}^H \sum_{(s, a) \in \mathcal{S} \times \mathcal{A}} \left| \left(\hat{P}_h^{\pi^E} \circ \mathcal{D}' \right) (s, a) - \sum_{\mathbf{tr}_h \in \text{Tr}_h^{\mathcal{D}_1}} \mathbb{P}^{\pi^E}(\mathbf{tr}_h) \mathbb{I}\{\mathbf{tr}_h(s_h, a_h) = (s, a)\} \right|}_{\text{Error A}} \\ + \underbrace{\sum_{h=1}^H \sum_{(s, a) \in \mathcal{S} \times \mathcal{A}} \left| \left(\hat{P}_h^{\pi^E} \circ \mathcal{D}_1^c \right) (s, a) - \sum_{\mathbf{tr}_h \notin \text{Tr}_h^{\mathcal{D}_1}} \mathbb{P}^{\pi^E}(\mathbf{tr}_h) \mathbb{I}\{\mathbf{tr}_h(s_h, a_h) = (s, a)\} \right|}_{\text{Error B}}.$$

We first analyze the term Error A. Recall that \mathcal{D}' is collected by the policy $\pi \in \Pi(\mathcal{D}_1)$ with $|\mathcal{D}'| = n$, and $\left(\hat{P}_h^{\pi^E} \circ \mathcal{D}' \right) (s, a)$ is an unbiased estimator for $\sum_{\mathbf{tr}_h \in \text{Tr}_h^{\mathcal{D}_1}} \mathbb{P}^{\pi^E}(\mathbf{tr}_h) \mathbb{I}\{\mathbf{tr}_h(s_h, a_h) = (s, a)\}$. Let E'_h^s be the event that \mathbf{tr}_h agrees with expert policy at state s at time step h and appears in $\text{Tr}_h^{\mathcal{D}_1}$. Formally,

$$E'_h^s = \mathbb{I}\{\mathbf{tr}_h(s_h, a_h) = (s, \pi_h^E(s)) \cap \mathbf{tr}_h \in \text{Tr}_h^{\mathcal{D}_1}\}.$$

By Lemma D.1, for each $s \in \mathcal{S}$ and $h \in [H]$, with probability at least $1 - \frac{\delta}{2|\mathcal{S}|H}$ over the randomness of \mathcal{D}' , we have

$$\left| \left(\hat{P}_h^{\pi^E} \circ \mathcal{D}' \right) (s, \pi_h^E(s)) - \sum_{\mathbf{tr}_h \in \text{Tr}_h^{\mathcal{D}_1}} \mathbb{P}^{\pi^E}(\mathbf{tr}_h) \mathbb{I}\{\mathbf{tr}_h(s_h, a_h) = (s, \pi_h^E(s))\} \right| \\ \leq \sqrt{\mathbb{P}^{\pi^E}(E'_h^s) \frac{3 \log(4|\mathcal{S}|H/\delta)}{n}}.$$

By union bound, with probability at least $1 - \frac{\delta}{2}$ over the randomness of \mathcal{D}' , we have

$$\text{Error A} \leq \sum_{h=1}^H \sum_{s \in \mathcal{S}} \sqrt{\mathbb{P}^{\pi^E}(E'_h^s) \frac{3 \log(4|\mathcal{S}|H/\delta)}{n}} \\ \leq \sum_{h=1}^H \sqrt{|\mathcal{S}|} \sqrt{\sum_{s \in \mathcal{S}} \mathbb{P}^{\pi^E}(E'_h^s) \frac{3 \log(4|\mathcal{S}|H/\delta)}{n}}$$

The last inequality follows the Cauchy-Schwarz inequality. It remains to upper bound $\sum_{s \in \mathcal{S}} \mathbb{P}^{\pi^E}(E'_h^s)$ for all $h \in [H]$. To this end, we define the event $G'_h^{\mathcal{D}_1}$ that expert policy π^E visits states covered in \mathcal{D}_1 up to time step h . Formally,

$G'_h^{\mathcal{D}_1} = \mathbb{I}\{\forall h' \leq h, s_{h'} \in \mathcal{S}_{h'}(\mathcal{D}_1)\}$, where $\mathcal{S}_h(\mathcal{D}_1)$ is the set of states in \mathcal{D}_1 at time step h . Then, for all $h \in [H]$, we have

$$\sum_{s \in \mathcal{S}} \mathbb{P}^{\pi^E}(E'_h^s) = \mathbb{P}^{\pi^E}(G'_h^{\mathcal{D}_1}) \leq \mathbb{P}(G'_1^{\mathcal{D}_1}).$$

The last inequality holds since $G'_h^{\mathcal{D}_1} \subseteq G'_1^{\mathcal{D}_1}$ for all $h \in [H]$. Then we have that

$$\text{Error A} \leq H \sqrt{\frac{3|\mathcal{S}| \log(4|\mathcal{S}|H/\delta)}{n}}.$$

When the interaction complexity satisfies that $n \gtrsim \frac{|\mathcal{S}|H^2}{\varepsilon^2} \log\left(\frac{|\mathcal{S}|H}{\delta}\right)$, with probability at least $1 - \frac{\delta}{2}$ over the randomness of \mathcal{D}' , we have $\text{Error A} \leq \frac{\varepsilon}{2}$. For the term Error B, we have analyzed it in the proof of Lemma 3.2. When the expert sample complexity satisfies that $m \gtrsim \frac{|\mathcal{S}|H^{3/2}}{\varepsilon} \log\left(\frac{|\mathcal{S}|H}{\delta}\right)$, with probability at least $1 - \frac{\delta}{2}$ over the randomness of \mathcal{D} , we have $\text{Error B} \leq \frac{\varepsilon}{2}$. Applying union bound finishes the proof. \square

Lemma E.2. *Consider the model-based transition-aware adversarial imitation learning approach displayed in Algorithm 2 and $\bar{\pi}$ is the output policy. Assume that in each iteration t , $\pi^{(t)}$ is ε_1 -optimal w.r.t reward function $w^{(t)}$ and true transition function \mathcal{P} , i.e.,*

$$\max_{\pi \in \Pi} V^{\pi, w^{(t)}} \leq V^{\pi^{(t)}, w^{(t)}} + \varepsilon_1, \quad (\text{E.1})$$

and the policy evaluation errors are upper bounded by ε_2 and ε_3 , respectively, i.e.,

$$|V^{\pi^{(t)}, \mathcal{P}, w^{(t)}} - V^{\pi^{(t)}, \hat{\mathcal{P}}, w^{(t)}}| \leq \varepsilon_2, \quad (\text{E.2})$$

$$|V^{\bar{\pi}, \mathcal{P}, w} - V^{\bar{\pi}, \hat{\mathcal{P}}, w}| \leq \varepsilon_3, \forall w \in \mathcal{W}, \quad (\text{E.3})$$

then we have

$$\begin{aligned} \sum_{h=1}^H \left\| P_h^{\bar{\pi}}(s, a) - \tilde{P}_h^{\pi^E}(s, a) \right\|_1 &\leq \min_{\pi \in \Pi} \sum_{h=1}^H \left\| P_h^{\pi}(s, a) - \tilde{P}_h^{\pi^E}(s, a) \right\|_1 \\ &\quad + 2H \sqrt{\frac{2|\mathcal{S}||\mathcal{A}|}{T}} + \varepsilon_1 + \varepsilon_2 + \varepsilon_3. \end{aligned}$$

Proof. Similar to the proof of Lemma D.4, we can obtain the dual representation of ℓ_1 -norm with the minimax theorem.

$$\min_{\pi \in \Pi} \sum_{h=1}^H \left\| P_h^{\pi}(s, a) - \tilde{P}_h^{\pi^E}(s, a) \right\|_1 = - \min_{w \in \mathcal{W}} \max_{\pi \in \Pi} \sum_{h=1}^H \sum_{(s, a) \in \mathcal{S} \times \mathcal{A}} w_h(s, a) \left(P_h^{\pi}(s, a) - \tilde{P}_h^{\pi^E}(s, a) \right).$$

Then we consider the term $\min_{w \in \mathcal{W}} \max_{\pi \in \Pi} \sum_{h=1}^H \sum_{(s, a) \in \mathcal{S} \times \mathcal{A}} w_h(s, a) \left(P_h^{\pi}(s, a) - \tilde{P}_h^{\pi^E}(s, a) \right)$.

$$\begin{aligned} &\min_{w \in \mathcal{W}} \max_{\pi \in \Pi} \sum_{h=1}^H \sum_{(s, a) \in \mathcal{S} \times \mathcal{A}} w_h(s, a) \left(P_h^{\pi}(s, a) - \tilde{P}_h^{\pi^E}(s, a) \right) \\ &\leq \max_{\pi \in \Pi} \sum_{h=1}^H \sum_{(s, a) \in \mathcal{S} \times \mathcal{A}} \left(\frac{1}{T} \sum_{t=1}^T w_h^{(t)}(s, a) \right) \left(P_h^{\pi}(s, a) - \tilde{P}_h^{\pi^E}(s, a) \right) \\ &\leq \frac{1}{T} \sum_{t=1}^T \max_{\pi \in \Pi} \sum_{h=1}^H \sum_{(s, a) \in \mathcal{S} \times \mathcal{A}} w_h^{(t)}(s, a) \left(P_h^{\pi}(s, a) - \tilde{P}_h^{\pi^E}(s, a) \right). \end{aligned}$$

Since $\pi^{(t)}$ is ε_1 -optimal w.r.t reward function $w^{(t)}$ and true transition function \mathcal{P} , then we have

$$\max_{\pi \in \Pi} \sum_{h=1}^H \sum_{(s, a) \in \mathcal{S} \times \mathcal{A}} w_h^{(t)}(s, a) P_h^{\pi}(s, a) = \max_{\pi \in \Pi} V^{\pi, w^{(t)}} \leq V^{\pi^{(t)}, w^{(t)}} + \varepsilon_1$$

$$= \sum_{h=1}^H \sum_{(s,a) \in \mathcal{S} \times \mathcal{A}} w_h^{(t)}(s,a) P_h^{\pi^{(t)}}(s,a) + \varepsilon_1.$$

Therefore, we obtain that

$$\begin{aligned} & \min_{w \in \mathcal{W}} \max_{\pi \in \Pi} \sum_{h=1}^H \sum_{(s,a) \in \mathcal{S} \times \mathcal{A}} w_h(s,a) \left(P_h^{\pi}(s,a) - \tilde{P}_h^{\pi^E}(s,a) \right) \\ & \leq \frac{1}{T} \sum_{t=1}^T \sum_{h=1}^H \sum_{(s,a) \in \mathcal{S} \times \mathcal{A}} w_h^{(t)}(s,a) \left(P_h^{\pi^{(t)}}(s,a) - \tilde{P}_h^{\pi^E}(s,a) \right) + \varepsilon_1. \end{aligned}$$

Furthermore, with the assumption that the policy evaluation error is upper bounded by ε_2 , we have

$$\left| \sum_{h=1}^H \sum_{(s,a) \in \mathcal{S} \times \mathcal{A}} w_h^{(t)}(s,a) \left(P_h^{\pi^{(t)}}(s,a) - \ddot{P}_h^{\pi^{(t)}}(s,a) \right) \right| = \left| V^{\pi^{(t)}, \mathcal{P}, w^{(t)}} - V^{\pi^{(t)}, \hat{\mathcal{P}}, w^{(t)}} \right| \leq \varepsilon_2,$$

where $\ddot{P}_h^{\pi^{(t)}}(s,a)$ and $\tilde{P}_h^{\pi}(s,a)$ are the state-action distribution of $\pi^{(t)}$ and $\bar{\pi}$ under the empirical transition function $\hat{\mathcal{P}}$, respectively. Then we obtain that

$$\begin{aligned} & \min_{w \in \mathcal{W}} \max_{\pi \in \Pi} \sum_{h=1}^H \sum_{(s,a) \in \mathcal{S} \times \mathcal{A}} w_h(s,a) \left(P_h^{\pi}(s,a) - \tilde{P}_h^{\pi^E}(s,a) \right) \\ & \leq \frac{1}{T} \sum_{t=1}^T \sum_{h=1}^H \sum_{(s,a) \in \mathcal{S} \times \mathcal{A}} w_h^{(t)}(s,a) \left(\ddot{P}_h^{\pi^{(t)}}(s,a) - \tilde{P}_h^{\pi^E}(s,a) \right) + \varepsilon_1 + \varepsilon_2 \\ & \leq \min_{w \in \mathcal{W}} \frac{1}{T} \sum_{t=1}^T \sum_{h=1}^H \sum_{(s,a) \in \mathcal{S} \times \mathcal{A}} w_h(s,a) \left(\ddot{P}_h^{\pi^{(t)}}(s,a) - \tilde{P}_h^{\pi^E}(s,a) \right) + \varepsilon_1 + \varepsilon_2 + 2H\sqrt{\frac{2|\mathcal{S}||\mathcal{A}|}{T}} \end{aligned} \quad (\text{E.4})$$

$$\begin{aligned} & = \min_{w \in \mathcal{W}} \sum_{h=1}^H \sum_{(s,a) \in \mathcal{S} \times \mathcal{A}} w_h(s,a) \left(\frac{1}{T} \sum_{t=1}^T \ddot{P}_h^{\pi^{(t)}}(s,a) - \tilde{P}_h^{\pi^E}(s,a) \right) + \varepsilon_1 + \varepsilon_2 + 2H\sqrt{\frac{2|\mathcal{S}||\mathcal{A}|}{T}} \\ & = \min_{w \in \mathcal{W}} \sum_{h=1}^H \sum_{(s,a) \in \mathcal{S} \times \mathcal{A}} w_h(s,a) \left(\ddot{P}_h^{\bar{\pi}}(s,a) - \tilde{P}_h^{\pi^E}(s,a) \right) + \varepsilon_1 + \varepsilon_2 + 2H\sqrt{\frac{2|\mathcal{S}||\mathcal{A}|}{T}} \end{aligned} \quad (\text{E.5})$$

$$\leq \min_{w \in \mathcal{W}} \sum_{h=1}^H \sum_{(s,a) \in \mathcal{S} \times \mathcal{A}} w_h(s,a) \left(P_h^{\bar{\pi}}(s,a) - \tilde{P}_h^{\pi^E}(s,a) \right) + \varepsilon_1 + \varepsilon_2 + \varepsilon_3 + 2H\sqrt{\frac{2|\mathcal{S}||\mathcal{A}|}{T}}, \quad (\text{E.6})$$

where (E.4) follows Lemma D.3, (E.5) follows that $\bar{\pi}$ is derived by the mean state-action distribution and (E.6) again utilizes the bound of policy evaluation error. Thus we have

$$\begin{aligned} & \min_{\pi \in \Pi} \sum_{h=1}^H \left\| P_h^{\pi}(s,a) - \tilde{P}_h^{\pi^E}(s,a) \right\|_1 \\ & = - \min_{w \in \mathcal{W}} \max_{\pi \in \Pi} \sum_{h=1}^H \sum_{(s,a) \in \mathcal{S} \times \mathcal{A}} w_h(s,a) \left(P_h^{\pi}(s,a) - \tilde{P}_h^{\pi^E}(s,a) \right) \\ & \geq - \min_{w \in \mathcal{W}} \sum_{h=1}^H \sum_{(s,a) \in \mathcal{S} \times \mathcal{A}} w_h(s,a) \left(P_h^{\bar{\pi}}(s,a) - \tilde{P}_h^{\pi^E}(s,a) \right) - \varepsilon_1 - \varepsilon_2 - \varepsilon_3 - 2H\sqrt{\frac{2|\mathcal{S}||\mathcal{A}|}{T}} \\ & = \max_{w \in \mathcal{W}} \sum_{h=1}^H \sum_{(s,a) \in \mathcal{S} \times \mathcal{A}} w_h(s,a) \left(\tilde{P}_h^{\pi^E}(s,a) - P_h^{\bar{\pi}}(s,a) \right) - \varepsilon_1 - \varepsilon_2 - \varepsilon_3 - 2H\sqrt{\frac{2|\mathcal{S}||\mathcal{A}|}{T}} \\ & = \sum_{h=1}^H \left\| P_h^{\bar{\pi}}(s,a) - \tilde{P}_h^{\pi^E}(s,a) \right\|_1 - \varepsilon_1 - \varepsilon_2 - \varepsilon_3 - 2H\sqrt{\frac{2|\mathcal{S}||\mathcal{A}|}{T}}, \end{aligned}$$

which completes the proof. \square

We then state the theoretical guarantee of RF-Express algorithm [Ménard et al., 2020], which is useful in proving the interaction complexity of Algorithm 2.

Theorem E.1 (Theorem 1 in [Ménard et al., 2020]). *Fix $\varepsilon \in (0, 1)$ and $\delta \in (0, 1)$. Consider the RF-Express algorithm and $\widehat{\mathcal{P}}$ is the empirical transition function built on the collected trajectories, if the number of collected trajectories satisfies*

$$n' \gtrsim \frac{H^3 |\mathcal{S}| |\mathcal{A}|}{\varepsilon^2} \left(|\mathcal{S}| + \log \left(\frac{|\mathcal{S}| H}{\delta} \right) \right).$$

Then with probability at least $1 - \delta$, for any policy π and any bounded reward function w between $[-1, 1]$, we have⁷ $|V^{\pi, \mathcal{P}, w} - V^{\pi, \widehat{\mathcal{P}}, w}| \leq \frac{\varepsilon}{2}$; furthermore, for any bounded reward function w between $[-1, 1]$, we have $\max_{\pi \in \Pi} V^{\pi, w} \leq V^{\widehat{\pi}_w^, w} + \varepsilon$, where $\widehat{\pi}_w^*$ is the optimal policy under empirical transition function $\widehat{\mathcal{P}}$ and reward function w .*

Proof of Theorem 4.1. First of all, we show that the assumptions in Lemma E.2 hold based on Theorem E.1 and derive the exact values of $\varepsilon_1, \varepsilon_2$ and ε_3 in the relevant assumptions. Then, we prove Theorem 4.1 based on Lemma E.1 and E.2.

In each iteration t of Algorithm 2, when $n' \gtrsim \frac{|\mathcal{S}| |\mathcal{A}| H^3}{\varepsilon^2} \left(|\mathcal{S}| + \log \left(\frac{|\mathcal{S}| H T}{\delta} \right) \right)$, by Theorem E.1, w.p. $\geq 1 - \frac{\delta}{4T}$, we have $|V^{\pi^{(t)}, \mathcal{P}, w^{(t)}} - V^{\pi^{(t)}, \widehat{\mathcal{P}}, w^{(t)}}| \leq \frac{\varepsilon}{16}$ and

$$\begin{aligned} V^{\pi^{(t)}, \mathcal{P}, w^{(t)}} &\geq V^{\pi^{(t)}, \widehat{\mathcal{P}}, w^{(t)}} - \frac{\varepsilon}{16} \geq V^{\widehat{\pi}_w^*, \widehat{\mathcal{P}}, w^{(t)}} - \frac{\varepsilon}{16} - \varepsilon_{\text{opt}} \geq V^{\pi_w^*, \widehat{\mathcal{P}}, w^{(t)}} - \frac{\varepsilon}{16} - \varepsilon_{\text{opt}} \\ &\geq V^{\pi_w^*, \mathcal{P}, w^{(t)}} - \frac{\varepsilon}{8} - \varepsilon_{\text{opt}} = \max_{\pi \in \Pi} V^{\pi, \mathcal{P}, w^{(t)}} - \frac{\varepsilon}{8} - \varepsilon_{\text{opt}}, \end{aligned}$$

where $\pi^{(t)}$ is the nearly optimal policy with an error of ε_{opt} under the empirical transition function $\widehat{\mathcal{P}}$ and reward function $w^{(t)}$, π_w^* and $\widehat{\pi}_w^*$ are the optimal policies under \mathcal{P} and $\widehat{\mathcal{P}}$, respectively. By union bound, for all $t \in [T]$, w.p. $\geq 1 - \frac{\delta}{4}$, we have

$$|V^{\pi^{(t)}, \mathcal{P}, w^{(t)}} - V^{\pi^{(t)}, \widehat{\mathcal{P}}, w^{(t)}}| \leq \frac{\varepsilon}{16} \quad \text{and} \quad V^{\pi^{(t)}, \mathcal{P}, w^{(t)}} \geq \max_{\pi \in \Pi} V^{\pi, \mathcal{P}, w^{(t)}} - \frac{\varepsilon}{8} - \varepsilon_{\text{opt}}.$$

For the policy $\bar{\pi}$ output by Algorithm 2, by Theorem E.1, w.p. $\geq 1 - \frac{\delta}{4}$, we have

$$\max_{w \in \mathcal{W}} |V^{\bar{\pi}, \mathcal{P}, w} - V^{\bar{\pi}, \widehat{\mathcal{P}}, w}| \leq \frac{\varepsilon}{16}.$$

In summary, we can set $\varepsilon_1 = \varepsilon_{\text{opt}} + \varepsilon/8, \varepsilon_2 = \varepsilon/16, \varepsilon_3 = \varepsilon/16$ in Lemma E.2. Then, by union bound, w.p. $1 - \frac{\delta}{2}$, we have

$$\sum_{h=1}^H \left\| P_h^{\bar{\pi}}(s, a) - \widetilde{P}_h^{\pi^{\text{E}}}(s, a) \right\|_1 \leq \min_{\pi \in \Pi} \sum_{h=1}^H \left\| P_h^{\pi}(s, a) - \widetilde{P}_h^{\pi^{\text{E}}}(s, a) \right\|_1 + 2H \sqrt{\frac{2|\mathcal{S}||\mathcal{A}|}{T}} + \frac{\varepsilon}{4} + \varepsilon_{\text{opt}}.$$

With Lemma E.1, with probability at least $1 - \frac{\delta}{2}$, when the number of expert demonstrations and the number of trajectories collected by $\pi \in \Pi(\mathcal{D}_1)$ satisfies that

$$m \gtrsim \frac{|\mathcal{S}| H^{3/2}}{\varepsilon} \log \left(\frac{|\mathcal{S}| H}{\delta} \right), \quad n \gtrsim \frac{|\mathcal{S}| H^2}{\varepsilon^2} \log \left(\frac{|\mathcal{S}| H}{\delta} \right),$$

we have $\sum_{h=1}^H \left\| \widetilde{P}_h^{\pi^{\text{E}}}(s, a) - P_h^{\pi^{\text{E}}}(s, a) \right\|_1 \leq \frac{\varepsilon}{8}$. Furthermore, when $T \gtrsim \frac{|\mathcal{S}||\mathcal{A}| H^2}{\varepsilon^2}$, we also have that $2H \sqrt{\frac{2|\mathcal{S}||\mathcal{A}|}{T}} \leq \frac{\varepsilon}{8}$. Combining the above inequalities, w.p. $1 - \delta$, we have that

$$\begin{aligned} \sum_{h=1}^H \left\| P_h^{\bar{\pi}}(s, a) - \widetilde{P}_h^{\pi^{\text{E}}}(s, a) \right\|_1 &\leq \min_{\pi \in \Pi} \sum_{h=1}^H \left\| P_h^{\pi}(s, a) - \widetilde{P}_h^{\pi^{\text{E}}}(s, a) \right\|_1 + 2H \sqrt{\frac{2|\mathcal{S}||\mathcal{A}|}{T}} + \frac{\varepsilon}{4} + \varepsilon_{\text{opt}} \\ &\leq \sum_{h=1}^H \left\| P_h^{\pi^{\text{E}}}(s, a) - \widetilde{P}_h^{\pi^{\text{E}}}(s, a) \right\|_1 + 2H \sqrt{\frac{2|\mathcal{S}||\mathcal{A}|}{T}} + \frac{\varepsilon}{4} + \varepsilon_{\text{opt}} \\ &\leq \frac{\varepsilon}{4} + \frac{\varepsilon}{4} + \frac{\varepsilon}{2} = \varepsilon. \end{aligned}$$

We finish the proof. \square

⁷This is implied by the stopping rule in RF-Express algorithm and Lemma 1 in [Ménard et al., 2020].

F Experiment Details

F.1 Known Transition Setting

We first consider the known transition setting. We use the optimal policy to collect expert demonstrations. The methods for comparison include BC [Pomerleau, 1991], GTAL [Syed and Schapire, 2007], FEM [Abbeel and Ng, 2004], OAL [Shani et al., 2021] and TAIL (see Algorithm 1). All methods are provided the same number of expert demonstrations. All experiments run with 20 random seeds. The detailed information on tasks is listed in Table 3. All experiments run on the machine with 32 CPU cores, 128 GB RAM and NVIDIA GeForce RTX 2080 Ti.

BC directly estimates the expert policy from expert demonstrations. The information on the number of iterations T of FEM, GTAL, OAL and TAIL is summarized in Table 4. In each iteration, with the recovered reward function, GTAL, FEM and our algorithm TAIL utilize value iteration to solve the optimal policy and OAL performs a policy mirror descent. As discussed in [Zahavy et al., 2020], the optimization problem of FEM can be solved by Frank Wolfe (FW) algorithm [Frank et al., 1956]. In particular, the step size of FW is determined by line search. GTAL [Syed and Schapire, 2007] uses multiplicative weights to solve the outer problem in (3.5). OAL and our algorithm TAIL utilize online gradient descent to update the reward function. To utilize the optimization structure, an adaptive step size [Orabona, 2019] is implemented for GTAL, OAL [Shani et al., 2021] and our algorithm TAIL⁸:

$$\eta_t = \frac{D}{\sqrt{\sum_{i=1}^t \|\nabla_w f^{(i)}(w^{(i)})\|_2^2}},$$

where $D = \sqrt{2H|\mathcal{S}||\mathcal{A}|}$ is the diameter of the set \mathcal{W} . After the training process, we evaluate the policy value via exact Bellman update. The running time of different algorithms on Reset Cliff is presented in Table 5. However, due to its computation issue, MIMIC-MD runs out of memory on the machine with 128 GB RAM when solving Reset Cliff with horizon exceeds 100.

Table 3: Information about tasks under known transition setting.

Tasks	Number of states	Number of actions	Horizon	Number of expert demonstrations
Standard Imitation (Figure 2a)	500	5	$10^1 \rightarrow 10^3$	300
Standard Imitation (Figure 2b)	500	5	10	$10^2 \rightarrow 10^4$
Reset Cliff (Figure 2c)	20	5	$10^1 \rightarrow 10^3$	5000
Reset Cliff (Figure 2d)	5	5	5	$10^2 \rightarrow 10^4$

Table 4: The number of iterations T of different algorithms on Standard Imitation and Reset Cliff.

Tasks	FEM	GTAL	OAL	TAIL
Standard Imitation (Figure 2a)	500	500	1400	500
Standard Imitation (Figure 2b)	8000	8000	8000	8000
Reset Cliff (Figure 2c)	300	300	300	300
Reset Cliff (Figure 2d)	20000	20000	20000	20000

Table 5: Running time of different algorithms on Reset Cliff. The unit is second.

Task	BC	FEM	GTAL	OAL	TAIL
Reset Cliff	1960.94 ± 369.05	2120.42 ± 451.09	2194.20 ± 452.88	1916.20 ± 107.99	2353.71 ± 488.59

F.2 Unknown Transition Setting

Under the unknown transition setting, the methods for comparison include OAL [Shani et al., 2021] and MB-TAIL. All experiments run with 20 random seeds. Table 6 summaries the detailed information on tasks under the unknown transition setting.

⁸Theoretical guarantee does not change by this adaptive step size [Orabona, 2019].

In particular, OAL is a model-based method and uses mirror descent (MD) [Beck and Teboulle, 2003] to optimize policy and reward. The step sizes of MD are set by the results in the theoretical analysis of [Shani et al., 2021]. During the interaction, OAL maintains an empirical transition model to estimate Q-function for policy optimization. To encourage exploration, OAL adds a bonus function to the Q-function. The bonus function used in the theoretical analysis of [Shani et al., 2021] is too big in experiments and hence, OAL requires too many interactions to reach a good and stable performance. Therefore, we simplify their bonus function from $b_h^k(s, a) = \sqrt{\frac{4H^2|\mathcal{S}|\log(3H^2|\mathcal{S}||\mathcal{A}|n/\delta)}{n_h^k(s, a)\vee 1}}$ to $b_h^k(s, a) = \sqrt{\frac{\log(H|\mathcal{S}||\mathcal{A}|n/\delta)}{n_h^k(s, a)\vee 1}}$, where n is the total number of interactions, δ is the failure probability and $n_h^k(s, a)$ is the number of times visiting (s, a) at time step h until episode k .

MB-TAIL first establishes the estimator in (4.1) with half of the environment interactions and learns an empirical transition model by invoking RF-Express [Ménard et al., 2020] to collect the other half of trajectories. Subsequently MB-TAIL performs policy and reward optimization with the recovered transition model. In MB-TAIL, the policy and reward optimization steps are the same as in TAIL.

Table 6: Information about tasks under unknown transition setting.

Tasks	Number of states	Number of actions	Horizon	Number of expert demonstrations
Reset Cliff	20	5	20	100
Standard Imitation	100	5	10	400

G Tightness of Theorem 3.1

Here we empirically validate that the sample complexity of TAIL presented in Theorem 3.1 is tight by empirical evaluations. In particular, we verify that the horizon dependency and sample complexity dependency of the policy value gap are $\tilde{\mathcal{O}}(H^{3/2})$ and $\tilde{\mathcal{O}}(1/m)$, respectively. We consider Three State MDP shown in Figure 6. Three State MDP is utilized to establish the lower bound of IL algorithms under the known transition setting in [Rajaraman et al., 2021]. The numerical result regarding the planning horizon is shown in Figure 5a. We see that the slope of TAIL w.r.t $\log(H)$ is around $3/2$, suggesting that the horizon dependency is $\tilde{\mathcal{O}}(H^{3/2})$. Besides, as shown in Figure 5b, we see that the slope w.r.t $\log(m)$ is about -1 , which indicates that the dependency on the number of expert demonstrations is $\tilde{\mathcal{O}}(1/m)$. In summary, we empirically verify that the sample complexity of TAIL is tight.

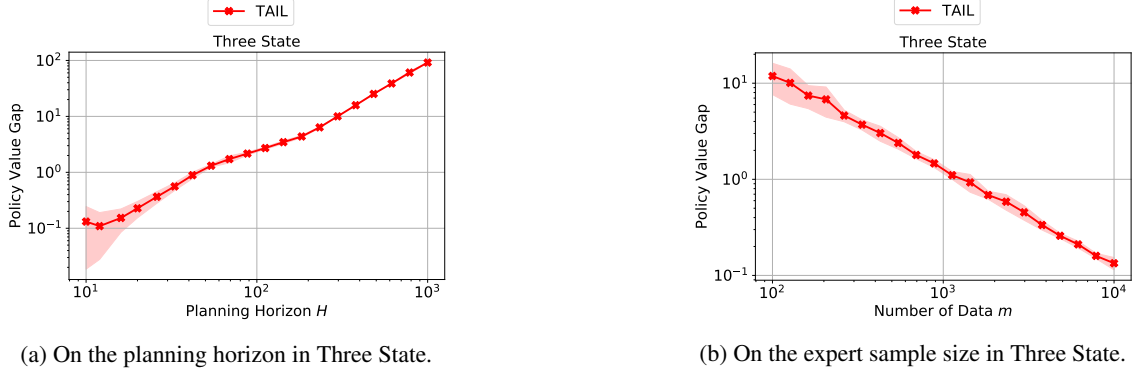


Figure 5: The policy value gap (i.e., $V^{\pi^E} - V^{\pi}$) in Three State with different planning horizons and the number of expert demonstrations.

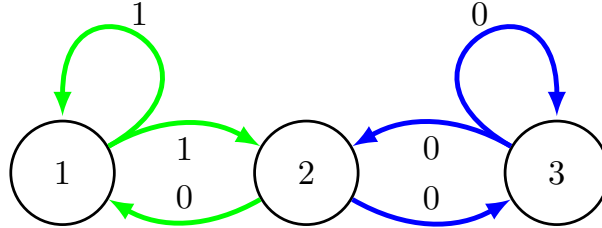


Figure 6: Three State MDP [Rajaraman et al., 2021]. There are two actions, shown in green and blue. There is only a single action on state 1 and 3. The expert policy always takes the green action. The initial state distribution is $\rho = (\rho(1), \rho(2), \rho(3)) = (1, 0, 0)$. Digits on arrows are corresponding rewards. When taking the only action on state 1 and 3, the agent goes to state 2 with a probability of $1/m$ and stays still with a probability of $1 - 1/m$. When taking the green action on state 2, the agent deterministically goes to state 1. Otherwise, the agent goes to state 3.